CHAPTER 2

Muscle-specific kinase myasthenia gravis IgG4 auto-antibodies cause severe neuromuscular junction dysfunction in mice

Rinse Klooster*, Jaap J. Plomp*, Maartje G. Huijbers, Erik H. Niks, Kirsten R. Straasheijm, Frank J. Detmers, Pim W. Hermans, Kevin Sleijpen, Aad Verrips, Mario Losen, Pilar Martinez-Martinez, Marc H. De Baets, Silvère M. van der Maarel, Jan J. Verschuuren

*Both authors contributed equally

Brain. 2012 Apr;135(Pt 4):1081-101.

ABSTRACT

Myasthenia gravis is a paralytic disorder with auto-antibodies against acetylcholine receptors at the neuromuscular junction. A proportion of patients instead has antibodies against muscle-specific kinase, a protein essential for acetylcholine receptor clustering. These are generally of the immunoglobulin-G4 subclass and correlate with disease severity, suggesting specific myasthenogenic activity. However, immunoglobulin-G4 subclass antibodies are generally considered to be 'benign' and direct proof for their pathogenicity in muscle-specific kinase myasthenia gravis (or other immunoglobulin-G4-associated disorders) is lacking. Furthermore, the exact electrophysiological synaptic defects caused at neuromuscular junctions by human anti-muscle-specific kinase auto-antibodies are hitherto unknown. We show that purified immunoglobulin-G4, but not immunoglobulin-G1-3, from patients with muscle-specific kinase myasthenia gravis binds to mouse neuromuscular junctions *in vitro*, and that injection into immunodeficient mice causes paralysis. Injected immunoglobulin-G4 caused reduced density and fragmented area of neuromuscular junction acetylcholine receptors. Detailed electrophysiological synaptic analyses revealed severe reduction of postsynaptic acetylcholine sensitivity, and exaggerated depression of presynaptic acetylcholine release during high-rate activity, together causing the (fatigable) muscle weakness. Intriguingly, compensatory transmitter release upregulation, which is the normal homeostatic response in acetylcholine receptor myasthenia gravis, was absent. This conveys extra vulnerability to neurotransmission at muscle-specific kinase myasthenia gravis neuromuscular junctions. Thus, we demonstrate that patient anti-muscle-specific kinase immunoglobulin-G4 is myasthenogenic, independent of additional immune system components, and have elucidated the underlying electrophysiological neuromuscular junction abnormalities.

INTRODUCTION

Myasthenia gravis is an autoimmune disease with antibodies against components of the neuromuscular junction causing fatigable muscle weakness. The most prevalent form of myasthenia gravis is caused by antibodies against the acetylcholine receptor (AChR), which induce damage of the postsynaptic membrane and defective neuromuscular transmission. A proportion of patients with myasthenia gravis (~5–10%) has antibodies against the postsynaptic transmembrane protein muscle-specific kinase (MuSK) (1). In complex with LRP4 and Tid1, this protein is involved in development and maintenance of AChR clustering under the influence of neural agrin (2,3,4,5). Although both forms of myasthenia gravis are caused by antibodies against neuromuscular junction components, there are several clinical, pharmacological and genetic arguments that separate them into two distinct disease entities (6,7,8,9). Notably, the immune response in MuSK myasthenia gravis is dominated by immunoglobulin (Ig)G4 auto-antibodies, instead of IgG1 or IgG3 in AChR myasthenia gravis (10,11,12,13), and anti-MuSK IgG4 but not IgG1–3 titres correlate with disease severity (14). The latter observation particularly suggests that pathogenic mechanisms differ between MuSK and AChR myasthenia gravis. IgG4 and IgG1–3 have different Fc (fragment, crystallizable) regions and will activate different immunological pathways (15). Human IgG1–3 is bivalent (enabling antigen cross-linking), activates complement and has strong pro-inflammatory properties. In contrast, IgG4 is functionally monovalent due to Fab (fragment, antigen binding) arm exchange (16), cannot activate complement and has low affinity for Fc receptors on immune cells, and has therefore been considered as benign and anti-inflammatory (17). In AChR myasthenia gravis, complement activation is indeed a major aspect of the antibody-mediated pathogenesis (18,19), while this seems not the case for MuSK myasthenia gravis (20,21).

After initial scepticism on the pathogenic role of MuSK myasthenia gravis IgG (20,21), a recent passive transfer study in mice has strongly indicated that MuSK myasthenia gravis IgG indeed contains the myasthenogenic factor (22). From this and further detailed experiments with MuSK myasthenia gravis whole-IgG, it has been postulated that the MuSK myasthenia gravis antibodies can dimerize, activate and internalize MuSK, which subsequently leads to reduction and dispersal of AChR clusters at the neuromuscular junction (23). These results, together with anti-MuSK IgG4 subclass being the predominant antibody in MuSK myasthenia gravis and the correlation of its titre with disease severity (14), suggest that anti-MuSK IgG4 antibodies are ultimately the myasthenogenic factor in MuSK myasthenia gravis serum. However, the human clinical studies provide only circumstantial evidence and there is no direct proof for this hypothesis. Furthermore, the exact electrophysiological defects at the neuromuscular junction induced by these antibodies are hitherto unknown.

Therefore, we performed passive transfer in mice with purified IgG4 and IgG1–3 fractions from plasma of patients with MuSK myasthenia gravis and characterized in detail their myasthenogenic effects with *in vivo* and *ex vivo* neuromuscular analyses.

To avoid immunity against injected human IgG and to exclude activation of immune pathways following antigenic binding of injected IgG we used NOD.CB17-Prkdc^{scid}/J (NOD/SCID) mice, which are immunodeficient due to lack of functional lymphoid cells and an incomplete complement system (24). The IgG4 but not the IgG1–3 fractions of patients with MuSK myasthenia gravis induced severe muscle weakness, which we demonstrate to be due to combined post- and presynaptic electrophysiological neuromuscular junction defects. Thus, we show that MuSK myasthenia gravis patient IgG4 auto-antibodies are directly myasthenogenic, independent of additional immune system components, and provide insight into their paralytic effect by elucidating the electrophysiological synaptic dysfunction these human auto-antibodies cause at single neuromuscular junction level.

MATERIALS AND METHODS

Patient material

Plasmapheresis fluid was obtained from therapeutic plasma exchange of four patients with MuSK myasthenia gravis, whom are clinically described in the supplementary material. Patients signed informed consent and the Medical Ethical Committee approved the study. Serum from two healthy individuals was obtained from Sanquin Blood Supply Foundation, Amsterdam, The Netherlands.

IgG4 and IgG1–3 purification

IgG4 and IgG1–3 were purified using a human IgG4 and a human total IgG-specific affinity resin (BAC BV, www.captureselect.com) on an AKTA explorer 900 (Pharmacia Biotech). The amount of plasma used per run was based on the IgG subtype concentrations, and the dynamic capacity of the column material, 6 and 15 mg/ml for the IgG4 and IgG total affinity resin, respectively. For both columns 25 ml affinity resin was used. The flow rate for all steps was set at 13 ml/min. Before addition of patient material, the column (XK 26) was equilibrated with 125 ml phosphate-buffered saline (PBS) pH 7.4. Thereafter, the plasma was diluted five times in citrate buffer and cleared from non-soluble material through a 0.22 µM filter (Millipore) and run through the anti-IgG4 column. The column was washed with 250 ml of PBS and bound material was eluted in 10 ml fractions with 375 ml 0.1 M glycine pH 3.0. These fractions were immediately neutralized with 1/10 volume 1 M Tris pH 8.0.

The non-bound fraction of the first purification step was again loaded on a regenerated 25 ml anti-IgG4 column to deplete all remaining IgG4. This IgG4 fraction was discarded and not used for the *in vitro* and *in vivo* experiments. A fraction of the IgG4 depleted plasma, depending on the total IgG content, was loaded on an anti-IgG total affinity resin using the same specifications as described above for the IgG4 affinity ligand.

Eluted fractions per purification containing high concentrations of IgG, based on OD280 measurements, were pooled and subsequently dialysed to PBS (molecular weight cut-off 3.5 kD), concentrated with a Vivaspin20 concentrator (Sartorius) and sterilized using a 0.22 µm filter (Millipore).

Sodium dodecyl sulphate-polyacrylamide gel electrophoresis and western blot analysis

Samples were loaded on an 8% sodium dodecyl sulphate–polyacrylamide gel using sample buffer without a reducing agent. Separated proteins were either stained with Coomassie brilliant blue or transferred to PVDF membrane (Millipore). Transfer efficiency was checked by incubation in ponceau S buffer [0.1% (w/v) ponceau S; 0.5% (v/v) acetic acid] for 1 min and subsequent washes with milli-Q water. Blots were thereafter blocked in 4% Marvel skimmed milk powder in PBS (Marvel-PBS) for 1 h at room temperature. Blocked membranes were incubated for 1 h at room temperature with primary antibody diluted in Marvel-PBS. As primary antibody the following antibodies were used: mouse anti-IgG1 (1:5000) (Sanquin), mouse anti-IgG2 (1:5000), mouse anti-IgG3 (1:5000) or mouse anti-IgG4 (1:5000) (Nordic Immunological laboratories). Membranes were washed five times in 0.05% Tween-20 (v/v) in PBS (PBS–Tween) and subsequently incubated for 1 h at room temperature with IRDye 800CW conjugated goat anti-mouse secondary antibody (1:5000) diluted in Marvel-PBS. Excess of antibody was removed by four washes with PBS–Tween followed by two washes in PBS. Bound antibodies were detected on the Odyssey (LI-COR Biosciences GmbH).

Anti-MuSK titre determination

MuSK titres (nM) were determined with a commercial radioimmunoassay (RSR Ltd) in the patient plasmas and the sera of the passive transfer mice, obtained at the end of the passive transfer period.

Mouse passive transfer studies

To circumvent the potential problem of a mouse immune response against repetitively injected human IgG we used immunodeficient NOD.CB17-Prkdc^{scid}/J mice (24). Original breeders were purchased from Jackson Laboratory (Bar Harbor). Mice were bred and housed in sterile individually ventilated cages in the Leiden University Medical Centre animal facilities. Sterilized food and drinking water were provided *ad libitum*. We used 29 female NOD/SCID mice, aged 4–5 weeks at the start, for passive transfer of purified subclass IgG from patients with MuSK myasthenia gravis. Details are provided in supplementary Table 1. After establishing baseline values for the *in vivo* neuromuscular tests (see below) during 2 days, the mice were daily injected intraperitoneally at ~10 a.m. with a dose of the purified subclass IgG dissolved in a volume of 333 µl sterile PBS (for exact dosing information see relevant 'Results' sections and supplementary Table 1).

Before the injection, the body weight of each mouse was determined and neuromuscular performance was assessed. If mice became very weak (score >1, see below) or body weight loss occurred of >20% compared with the starting weight, or >15% in 1–2 consecutive days, passive transfer was terminated and mice were directly subjected to electromyographical testing, followed by CO_2 euthanasia and dissection of muscle nerve preparations for *ex vivo* neuromuscular junction

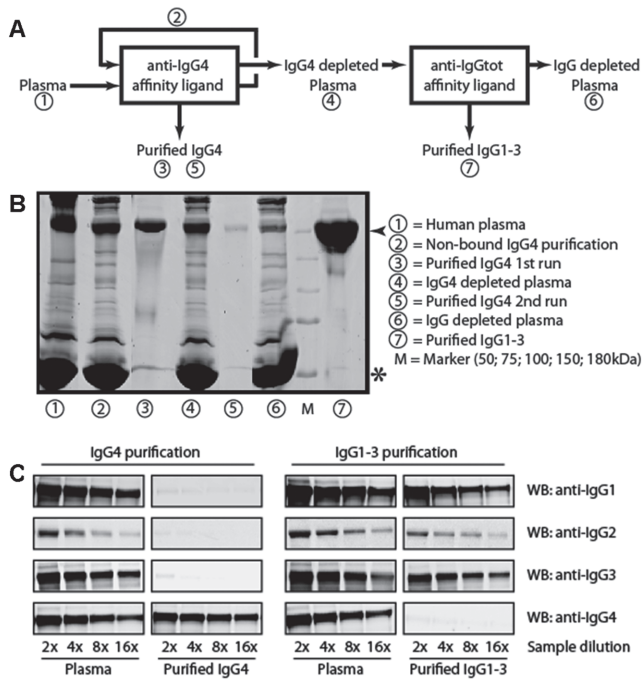

Figure 1. Purification of subclass IgG. (A) Schematic representation of the IgG subtype purification pipeline, in which plasmapheresis fluid is run over the IgG4 affinity resin two consecutive times to purify and deplete IgG4, followed by a run over the IgGtotal affinity resin to purify the remaining IgG1–3. (B) Representative results of the IgG4 and IgG1–3 purification of Patient 3 analysed on a Coomassie-stained gel to assess the purification of the IgG fractions (arrowhead indicates molecular weight of IgG; asterisk indicates molecular weight of human serum albumin). (C) Representative western blot of Patient 4 to assess the efficiency of depletion and purity of the IgG fractions. Only minimal reciprocal contamination of the different IgG subclass fractions was observed.

function tests and histology. All experiments were carried out according to Dutch law and Leiden University guidelines, including approval by the local Animal Experiments Committee.

In vivo assessment of neuromuscular function

Weakness in mice was visually scored (0 = no weakness, 1 = weakness upon activity, 2 = weakness at rest, 3 = severe weakness with breathing difficulty, 4 = death) (25). Forelimb and abdominal muscle strength was tested using a grip strength meter (type 303500, Technical and Scientific Equipment GmbH). The average peak force value of a trial of 10 consecutive pulls was calculated. The inverted mesh hanging test was used to assess fatigability of limb and abdominal muscles as described before (26). The test ended upon falling or completing the maximum hanging time, which was set at 120 s. Respiratory rate and tidal amplitude were assessed with non-invasive whole-body plethysmography in unrestrained animals (RM-80, Columbus Instruments). The signal was digitized using a Minidigi digitizer and Axoscope 10 (Axon Instruments/

Molecular Devices) and analysed with the event detection feature of Clampfit 9.2 (Axon Instruments/Molecular Devices).

Repetitive nerve stimulation electromyography

Mice were anaesthetized with a 1.5:1 (v/v) mixture of ketamine hydrochloride (Nimatek; 100 mg/ml, Eurovet) and medetomidine hydrochloride (Domitor; 1 mg/ml, Pfizer), at 1.25 µl/g mouse body weight, adjusted with Ringer solution to 200 µl volume and administered intraperitoneally. Mice were maintained at 37°C on a heating pad. A grounding needle electrode was inserted subcutaneously in the right thigh. Stimulation needle electrodes were inserted near the sciatic nerve in the left leg thigh. Subcutaneous recording needle electrodes were inserted near the calf muscles of the left leg. Grounding and recording electrodes were coupled via an AI402 pre-amplifier to a Cyberamp-380 signal conditioner (Axon Instruments/Molecular Devices). The nerve was stimulated supramaximally from a computer-controlled programmable electrical stimulator (AMPI). Trains of 10 stimuli were applied at increasing frequencies of 0.2, 1, 3, 5, 10, 20 and 40 Hz, with a 10–30 s pause between trains. Compound muscle action potentials (CMAPs) were digitized using a Digidata 1440 interface (Axon Instruments/Molecular Devices) and peak–peak amplitudes were determined in Clampfit 9.2 (Axon Instruments/Molecular Devices). After completing the recordings, mice were sacrificed by CO_2 inhalation without recovery from anaesthesia and muscles were dissected for the studies described below.

Ex vivo muscle contraction studies

Contraction force of left phrenic nerve-hemidiaphragms was recorded in Ringer's medium containing (in mM): NaCl 116, KCl 4.5, $CaCl_2$ 2, $MgCl_2$ 1, NaH_2PO_4 1, $NaHCO_3$ 23, glucose 11, pH 7.4) at room temperature (20–22°C) with a force transducer (type K30, Harvard Apparatus, Hugo Sachs Elektronik GmbH), connected to an amplifier TAM-A 705/1 (Hugo Sachs Elektronik). The signal was digitized using a Digidata 1440 digitizer (Axon Instruments/Molecular Devices), connected to a PC running Axoscope 10 (Axon Instruments). The phrenic nerve was stimulated supramaximally once every 5 min with 120 stimuli at 40 Hz. The safety factor of neuromuscular transmission was assessed by measuring contraction force in the presence of various concentrations (15–1000 nM) d-tubocurarine (Sigma-Aldrich). The amplitude of the recorded contractions was cursor-measured in Axoscope, at 2 s after the start.

Ex vivo neuromuscular junction electrophysiology

Intracellular recordings of miniature endplate potentials and endplate potentials at the neuromuscular junction were made in Ringer's solution at 26–28°C in right phrenic nerve-hemidiaphragm preparations. Just lateral of the main intramuscular phrenic nerve branch, muscle fibres were impaled with a glass microelectrode (10–20 MΩ, filled with 3 M KCl) connected to a Geneclamp 500B (Axon Instruments/Molecular devices) for amplifying and filtering (10 kHz low-pass). Although at the used low (×40)

light-microscopical magnification neuromuscular junctions are not directly visible (but the electrode-tip is), we know from fluorescence microcopical studies that neuromuscular junctions are strictly localized in that area. In controls, ~100% of the impalements yields synaptic signals with kinetical characteristics (i.e. a 0–100% rise time <2 ms) that assure correct placement of the electrode near the neuromuscular junction. The signal was digitized using a Digidata 1322A (Axon Instruments/Molecular Devices) and analysed using Clampfit 9.2 (Axon Instruments/Molecular Devices) and Mini Analysis 6.0.3 (Synaptosoft). Muscle action potentials were eliminated by using the skeletal muscle Na^+ channel blocker, μ-Conotoxin GIIIB (3 μM) (Scientific Marketing Associates). To record endplate potentials, the phrenic nerve was stimulated using a bipolar platinum electrode connected via an optical stimulus isolation unit to a computer-controlled programmable electrical stimulator (AMPI). Mean endplate potential and miniature endplate potential amplitudes at each neuromuscular junction were normalized to −75 mV, with the reversal potential for acetylcholine-induced current assumed 0 mV (27). To calculate the quantal content for each neuromuscular junction, the mean amplitude of the 20 endplate potentials recorded at low rate (0.3 Hz) stimulation were corrected for non-linear summation (28) and the normalized and corrected mean endplate potential amplitude was divided by the normalized mean miniature endplate potential amplitude (calculated from at least 20 miniature endplate potentials sampled). The quantal content is the number of acetylcholine quanta that is released upon a single nerve impulse. In each muscle, 40–60 muscle fibres were impaled to determine the percentage of neuromuscular junctions that were synaptically active or 'silent' (i.e. showing no miniature endplate potentials and no muscle action potential upon nerve stimulation). Thereafter, μ-Conotoxin GIIIB was applied and allowed to paralyze the preparation (usually within 15 min). Then, a measuring session of 20 endplate potentials evoked at 0.3 Hz nerve stimulation, spontaneous miniature endplate potentials during 2 min and a train of 35 endplate potentials at 40 Hz nerve stimulation was performed at 8–15 single neuromuscular junctions randomly sampled within the muscle.

Fluorescence microscopy of neuromuscular junctions

We assessed the binding capacity of purified patient IgG subclass fractions at the neuromuscular junction in muscle strips of dissected sets of small and thin cranial muscles from normal C57bl6/j mice, collectively referred to as levator auris longus, since most strips were from that particular muscle, but strips were also included of the closely underlying muscles (auricularis superior, abductor auris longus and interscutularis). These muscles are flat and thin and therefore exceptionally suitable for neuromuscular junction whole-mount imaging studies (29). Strips were fixed for 30 min at room temperature in 1% paraformaldehyde in PBS. After washing 30 min in PBS and incubating 30 min in 3% bovine serum albumin in PBS, muscles were incubated overnight at 4°C in 1:100 dilution of the purified IgGs from human MuSK myasthenia gravis Patients 1–3 and normal human control subjects. Samples were

washed for 1 h at room temperature with PBS, and subsequently incubated for 2.5 h at room temperature in a combination solution in PBS of 1:100 Alexa Fluor 546-conjugated goat anti-human IgG (Invitrogen) and 1 µg/ml Alexa Fluor 488 conjugated α-bungarotoxin (Invitrogen), followed by a PBS wash for 1 h. Muscle strips were mounted on microscope slides with Citifluor AF-1 antifadent and viewed under a Zeiss LSM 7 MP laser scanning microscope using a ×20 water immersion objective.

We also analysed morphology of neuromuscular junctions in diaphragm and levator auris longus muscles of the passively transferred mice. Diaphragm strips were fixed in 1% paraformaldehyde in PBS, washed in PBS and incubated for 3.5 h with 1µg/ml Alexa Fluor 488 conjugated α-bungarotoxin, followed by PBS wash (30 min), all at room temperature. AChR receptor staining at diaphragm neuromuscular junctions was quantified using ImageJ v1.44 (http://rsbweb.nih.gov/ij/). Ten randomly chosen neuromuscular junctions in the vertical midline of each of the lower-magnification pictures were selected and neuromuscular junction area was defined using the thresholding feature of the program. For each neuromuscular junction we determined stained area, mean pixel intensity and summed intensity (i.e. area multiplied by mean intensity). The mean ± SEM of these values was calculated for each picture. Differences were statistically tested with ANOVA and *post hoc* Tukey test. Levator auris longus neuromuscular junctions were incubated overnight at 4°C with rabbit anti-synaptic vesicle protein 2 (SV2) IgG antibody (produced from hybridoma cells purchased from The Developmental Studies Hybridoma Bank from the University of Iowa, USA), followed by PBS wash (30 min), Alexa Fluor 546-conjugated goat anti-rabbit IgG (Invitrogen) incubation for 2.5 h and again 30 min PBS wash (all at room temperature). Muscles were whole-mounted and viewed under the confocal laser scanning microscope.

Electron microscopy

Ultrastructural neuromuscular junction analysis was performed as described (30). Briefly, diaphragm muscles were fixed in 2.5% glutaraldehyde and 2% paraformaldehyde in PBS for 1 h at 4°C, post-fixed with 1% osmium tetroxide, dehydrated through a graded ethanol series and embedded in epoxy resin. Ultrathin sections were viewed with a Philips CM 100 electron microscope. At least six endplate regions were photographed per muscle. Quantitative morphometry of the folding index (length of postsynaptic membrane/length of presynaptic membrane) was performed as described (31,32).

Statistical tests

Wherever appropriate, Student's *t*-test or ANOVA with Tukey's *post hoc* test were performed, as indicated. Differences with *P*-values < 0.05 were considered statistically significant.

RESULTS

Purification of IgG4 and IgG1–3

Using VHH-based affinity resins, we purified IgG1–3 and IgG4 from plasmapheresis fluid of four patients with MuSK myasthenia gravis (clinically described in the supplementary material) and from pooled serum of two healthy individuals, using IgG subclass-specific affinity chromatography (Fig. 1A). Only minimal contamination with other proteins remained in both the IgG4 and the IgG1–3 fractions in a Coomassie-stained gel (Fig. 1B). Western blots demonstrated almost complete absence of IgG4 in the IgG1–3 fraction, and of IgG1, 2 and 3 in the IgG4 fraction (Fig. 1C). The minimal enrichment of IgG4 compared with the IgG4/IgG1–3 ratio in the starting plasma sample was ~200 times, which may be an underestimation due to the possibility that the secondary IgG subclass-specific antibodies used for detection may have some degree of cross-reactivity (12).

Selective binding of IgG4 from patients with MuSK myasthenia gravis to the neuromuscular junction

In levator auris longus muscles from untreated C57Bl6/J mice we assessed the neuromuscular junction binding potency of purified patient IgG4 and IgG1–3. Muscles were incubated with IgG and with fluorescently labelled α-bungarotoxin, which binds to AChRs and thus delineates the neuromuscular junction. Confocal laser scanning microscopy showed clearly co-localized IgG and AChR staining in preparations incubated with the purified IgG4 fractions from the three patients, while there was no IgG staining with patient IgG1–3 fractions or purified normal human IgG4 (Fig. 2). This shows that IgG4 of patients with MuSK myasthenia gravis selectively binds to the neuromuscular junction.

Passive transfer of purified IgG4 from patients with MuSK myasthenia gravis induces muscle weakness in mice

We injected young female NOD/SCID mice with different daily doses of MuSK myasthenia gravis IgG4 (14 mice) and IgG1–3 (8 mice). For details see supplementary Table 1. Daily injection of mice with 4 mg (from Patients 1 and 2), 0.5 mg or more (Patient 3) and 4 mg or more (Patient 4) purified MuSK myasthenia gravis IgG4 caused progressive body weight loss and overt muscle weakness (visual scoring grade 1–2), starting after ~1 week (Fig. 3A). We quantified the (fatigable) muscle weakness with

Figure 2. Demonstration of the selective binding of MuSK myasthenia gravis IgG4 to neuromuscular junctions. Maximum intensity projections of confocal laser scanning microscopical images of mouse levator auris longus neuromuscular junctions co-stained for AChRs with Alexa Fluor 488 α-bungarotoxin (green) and with purified MuSK myasthenia gravis patient IgG4, IgG1–3 or purified normal human IgG4 (all in red). The IgG4 from each of the three tested patients with MuSK myasthenia gravis stained the neuromuscular junction, while IgG staining at neuromuscular junctions was absent with the matched IgG1–3 fractions or normal human IgG4.

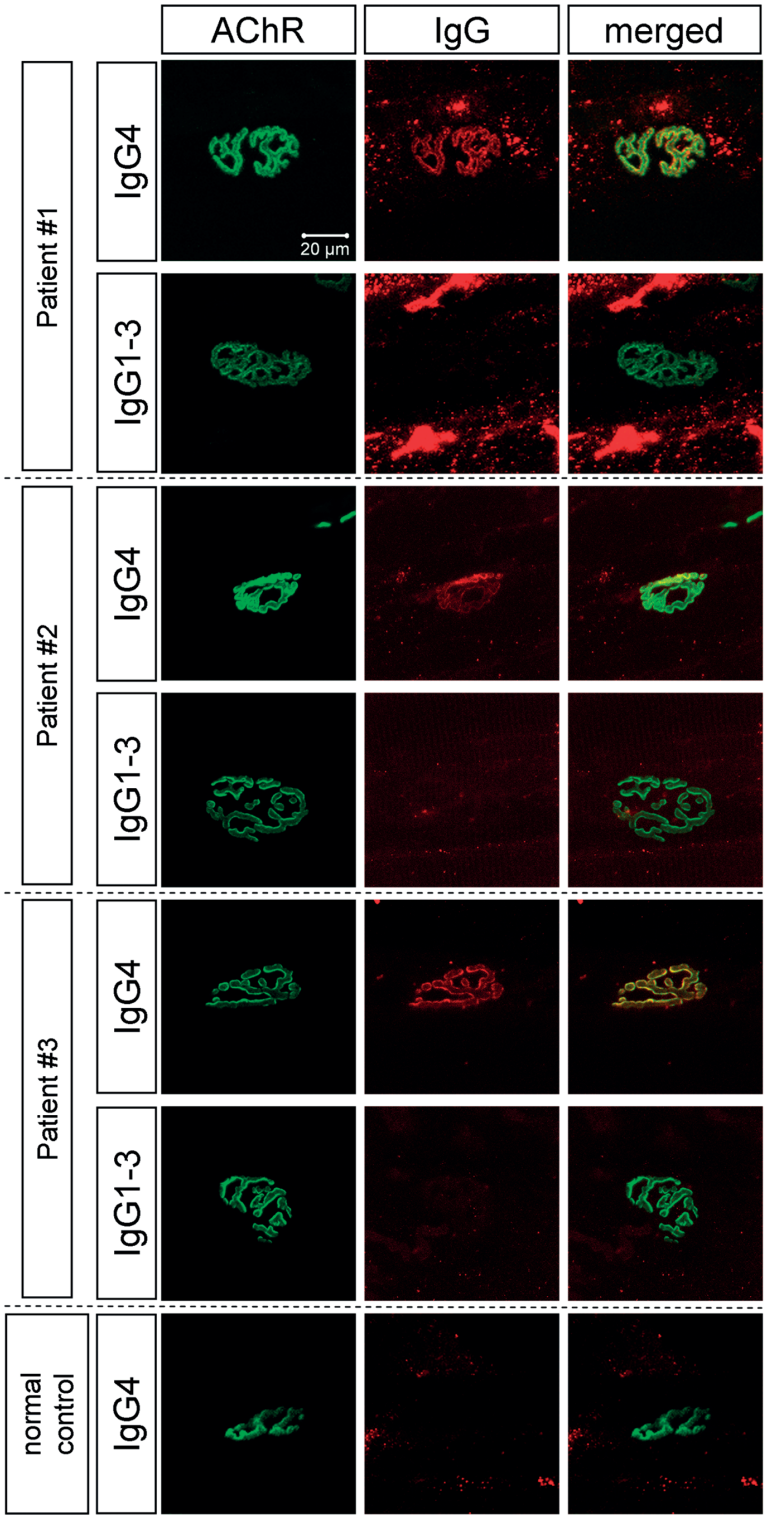
AChR
IgG
merged
Patient #1
IgG4
IgG1-3
20 µm
Patient #2
IgG4
IgG1-3
Patient #3
IgG4
IgG1-3
normal control
IgG4

grip strength and inverted mesh testing. After ~10 days of injection, the affected mice pulled <20–25% of the initial force (Fig. 3D) and fell off the inverted mesh in ~0–40 s, much faster than initially when they completed the allowed 120 s hanging time (Fig. 3G). Concomitant progressive reduction of tidal volume, detected in whole-body plethysmography, suggested increasing weakness of breathing muscles (Fig. 2J). In total, we observed 10 clinically weak mice after receiving MuSK myasthenia gravis IgG4 injection (supplementary Table 1). Eight control NOD/SCID mice that received 4 mg/day purified IgG1–3 of the same four patients with MuSK myasthenia gravis (two mice per patient IgG1–3 tested, supplementary Table 1) showed no such body weight loss or (fatigable) muscle weakness (Fig. 3), nor did control NOD/SCID mice that received either 4 mg/day normal human IgG4 or only the vehicle, PBS (Fig. 3).

At the end of the experiment, anti-MuSK antibodies in the serum of the mice treated with IgG4 reached levels 5–10 times higher than those in the patient plasmas, while no anti-MuSK reactivity could be detected in the IgG1–3 injected mice or the mouse injected with 4 mg/day healthy control IgG4 (supplementary Table 2).

Depending on the patient material, lower daily doses IgG4 (0.13–1.5 mg) caused no *in vivo* weakness but showed subclinical weakness (in muscle contraction tests and neuromuscular junction electrophysiological experiments, supplementary Fig. 2).

After ending passive transfer, *in vivo* neuromuscular junction function was assessed in calf muscles with repetitive nerve stimulation electromyography at various frequencies (0.2–40 Hz, 10 stimuli per frequency). All of the clinically weak MuSK myasthenia gravis IgG4-treated mice tested showed considerable reduction of CMAPs (Fig. 4 and supplementary Table 1), indicating progressive loss of successfully transmitting neuromuscular junctions during stimulation and explaining the observed fatigable muscle weakness. CMAP reduction depended on stimulation frequency, becoming apparent from 3 Hz stimulation and maximizing at frequencies of ≥10 Hz. CMAP reductions at 10 Hz stimulation ranged from ~20% (Mouse 2, passively transferred with Patient 1 IgG4, to almost 100% in Mouse 9, treated with Patient 2 IgG4 (supplementary Table 1). Figure 4C shows 10 consecutive CMAPs recorded at 10 Hz in Patient 2 IgG4-treated Mouse 5, decrementing by ~70%. No CMAP reduction was found in the control NOD/SCID mice, injected with either MuSK myasthenia gravis IgG1–3, normal human IgG4 or PBS. On average, 10 Hz stimulation resulted in 51.5 ± 10% CMAP amplitude decrement in the clinically weak MuSK myasthenia gravis mice tested ($n = 8$), whereas IgG1–3-treated control NOD/SCID mice ($n = 8$) showed 3.1 ± 0.7 increment ($P < 0.001$, Student's t-test, Fig. 4D).

MuSK myasthenia gravis IgG4 disturbs synaptic transmission at the neuromuscular junction

In *ex vivo* contraction experiments we tested muscle strength, fatigability and the safety factor of neuromuscular transmission in muscles of the passively transferred mice. Mean force delivered upon 40 Hz tetanic nerve stimulation by hemidiaphragms of patient IgG4-injected mice was 10.8 ± 0.9 g, while that of pooled controls was

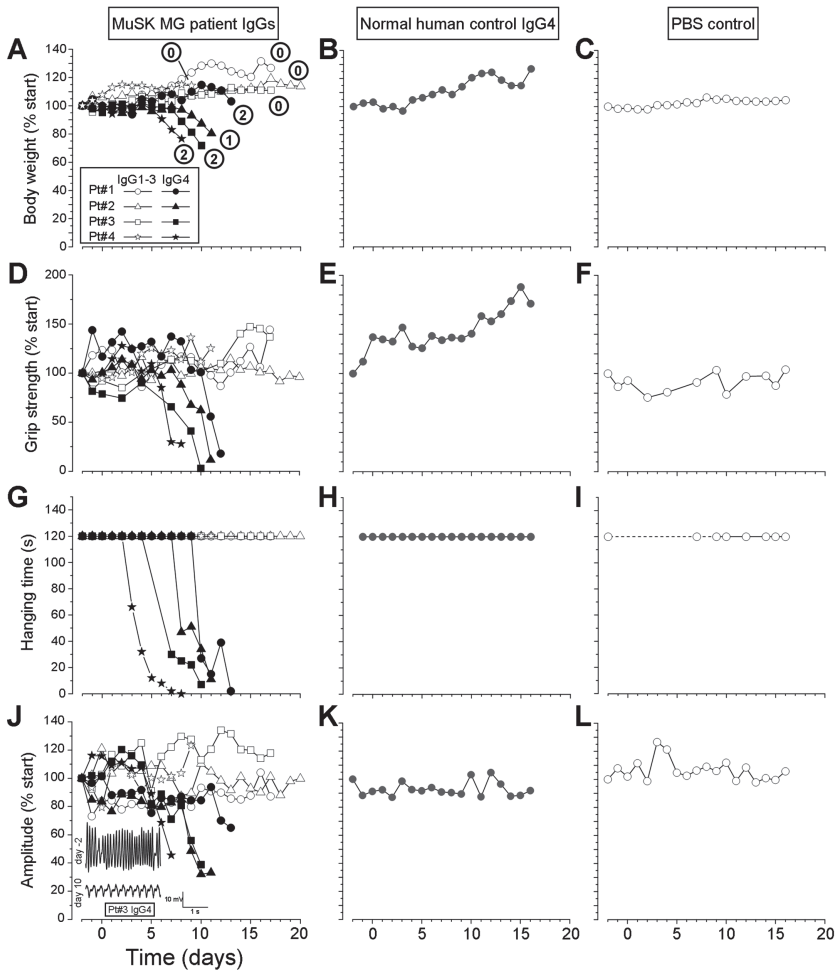

Figure 3. Passive transfer of MuSK myasthenia gravis IgG4 into NOD/SCID mice causes clinical myasthenia gravis. Exemplary *in vivo* neuromuscular tests of four individual young (3–5 weeks old) female NOD/SCID mice each injected with MuSK myasthenia gravis (MG) IgG4 from a different patient (4 mg/day, Patient 1, 2 and 4 or 2 mg/day, Patient 3) and four NOD/SCID mice, each injected with IgG1–3 from the same patients (all 4 mg/day), one NOD/SCID mouse injected with normal human IgG4 (4 mg/day, pooled from two healthy donors) and one NOD/SCID mouse injected with 333 µl PBS alone. For overview of all injected NOD/SCID mice of this study, see supplementary Table 1. Baseline was determined 2 days before start of injections (on Day 0). (A–C) Body-weight loss of the MuSK myasthenia gravis IgG4 mice and muscle weakness score of ≥1 at the end of the experiment (encircled values). All controls showed neither body-weight loss nor muscle weakness (all scored 0). (D–F) Grip-strength became severely diminished in MuSK myasthenia gravis IgG4 mice. (G–I) Inverted mesh hanging-time became much shorter for MuSK myasthenia gravis IgG4 mice. All control mice completed the maximum period (2 min). The PBS-injected mouse initially showed some premature falls (dashed line) due to excessive exploratory behaviour, but later completed the test, when MuSK myasthenia gravis IgG4-injected mice failed. (J–L) Respiration amplitude of MuSK myasthenia gravis IgG4-injected mice became reduced. Inset in J shows recorded signals before treatment and after 10 days injection with Patient 3 IgG4. Respiration amplitude of all control mice remained stable.

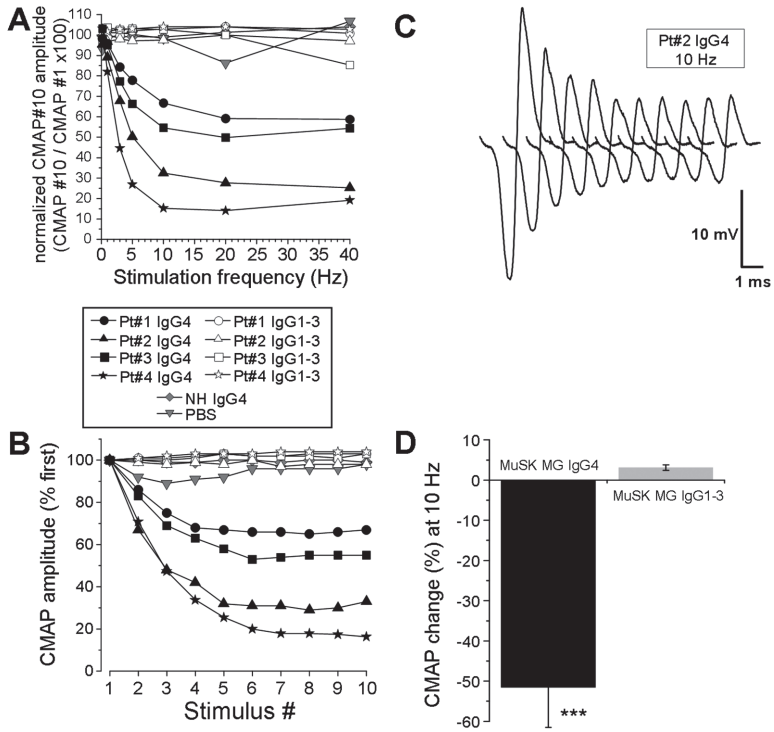

Figure 4. Passive transfer of MuSK myasthenia gravis IgG4 causes severe CMAP reduction. Repetitive nerve stimulation electromyography in anaesthetized mice revealed frequency-dependent reduction of CMAPs, compatible with a myasthenia gravis-like neuromuscular junction defect. (A) Stimulation frequency-dependency of CMAP decrements in the same exemplary mice as used for Fig. 3. (B) Development of CMAP amplitude during 10 stimuli at 10 Hz. (C) Example CMAPs in a mouse injected with Patient 2 IgG4. (D) Group comparison of CMAP amplitude change during 10 Hz nerve stimulation. ***$P < 0.001$, clinically weak MuSK myasthenia gravis IgG4 ($n = 8$ mice) versus MuSK myasthenia gravis IgG1–3 ($n = 8$ mice).

17.6 ± 0.5 g ($P < 0.001$, Student's t-test, n = 10 and 8 mice, respectively; for example contraction profiles see Fig. 5A). Tetanic fade (i.e. rundown of contraction force in spite of continuous nerve stimulation) was observed with most (8/10) muscles from the clinically weak mice injected with MuSK myasthenia gravis IgG4. Next, muscles were exposed to several concentrations of the reversible AChR antagonist d-tubocurarine and the inhibiting effect on tetanic contraction force was determined. Hemidiaphragms of the 10 clinically weak mice injected with MuSK myasthenia gravis patient IgG4 were more sensitive, with (intrapolated) 50% inhibiting d-tubocurarine concentrations of ~50 nM, while that of the eight MuSK myasthenia gravis IgG1–3, one normal human IgG4 and two PBS-injected controls was ~400 nM (Fig. 5B, $P < 0.001$, MuSK myasthenia gravis IgG4 versus IgG1–3, Student's t-test). This shows that MuSK myasthenia gravis IgG4 severely reduces the safety factor of neuromuscular transmission at the neuromuscular junction.

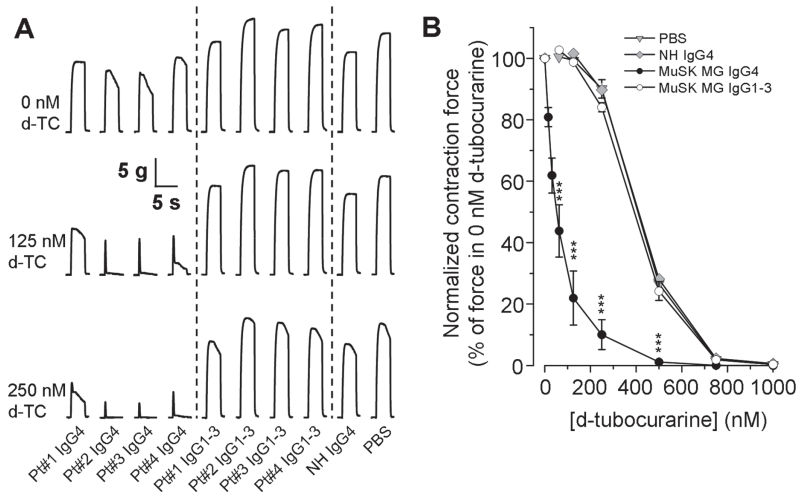

Figure 5. Passive transfer of MuSK myasthenia gravis IgG4 causes tetanic fade and reduced safety factor of neuromuscular transmission. Contraction experiments on left hemidiaphragm from passive transfer mice. (A) Example muscles from mice injected with Patient 1–4 IgG4, three of them showing tetanic fade upon 40 Hz nerve stimulation (upper row of traces). All MuSK myasthenia gravis IgG4 muscles delivered a lower absolute force as compared with the controls and were much more sensitive to reduction of force by the reversible AChR antagonist d-tubocurarine (d-TC). Examples of the contraction profiles in the presence of 125 and 250 nM are shown in the second and third row of traces. (B) Concentration–effect relationship of d-tubocurarine and contraction force, showing a large leftward shift of the curves of the muscles of 10 tested clinically weak mice injected with MuSK myasthenia gravis IgG4 (from an estimated EC_{50} of ~400 nM in controls to ~50 nM), demonstrating greatly reduced safety factor of neuromuscular transmission at neuromuscular junctions. ***$P < 0.001$, clinically weak MuSK myasthenia gravis IgG4 ($n = 10$ mice) versus MuSK myasthenia gravis IgG1–3 ($n = 8$ mice).

To elucidate the exact transmission defects at the neuromuscular junction underlying the fatigable muscle weakness caused by MuSK myasthenia gravis IgG4, we performed detailed ex vivo electrophysiological studies. Micro-electrode recordings of synaptic signals at neuromuscular junctions of diaphragm muscles from the NOD/SCID mice injected with IgG4 revealed small mean miniature endplate potential amplitudes (on average 0.67 ± 0.09 mV, i.e. ~50% reduction), as compared with 1.31 ± 0.03 mV observed in IgG1–3 injected NOD/SCID controls ($P < 0.001$, Student's t-test, $n = 10$ and 8 mice, respectively; Fig. 6A–D). Miniature endplate potentials occurred considerably less frequently (−55%) at neuromuscular junctions from all weak MuSK myasthenia gravis patient IgG4-treated mice, being on average 0.29 ± 0.02 s, compared with 0.65 ± 0.03/s in controls ($P < 0.001$; Fig. 6E). In addition, there was more amplitude variation amongst miniature endplate potentials recorded at individual neuromuscular junctions in muscles from weak mice injected with IgG4 from Patients 1, 2 and 4, group mean variance coefficients 0.39 ± 0.02 compared with 0.29 ± 0.01 in IgG1–3 NOD/SCID controls ($P < 0.001$; Fig. 6F). Furthermore, there was a tendency of slowed miniature endplate potential kinetics,

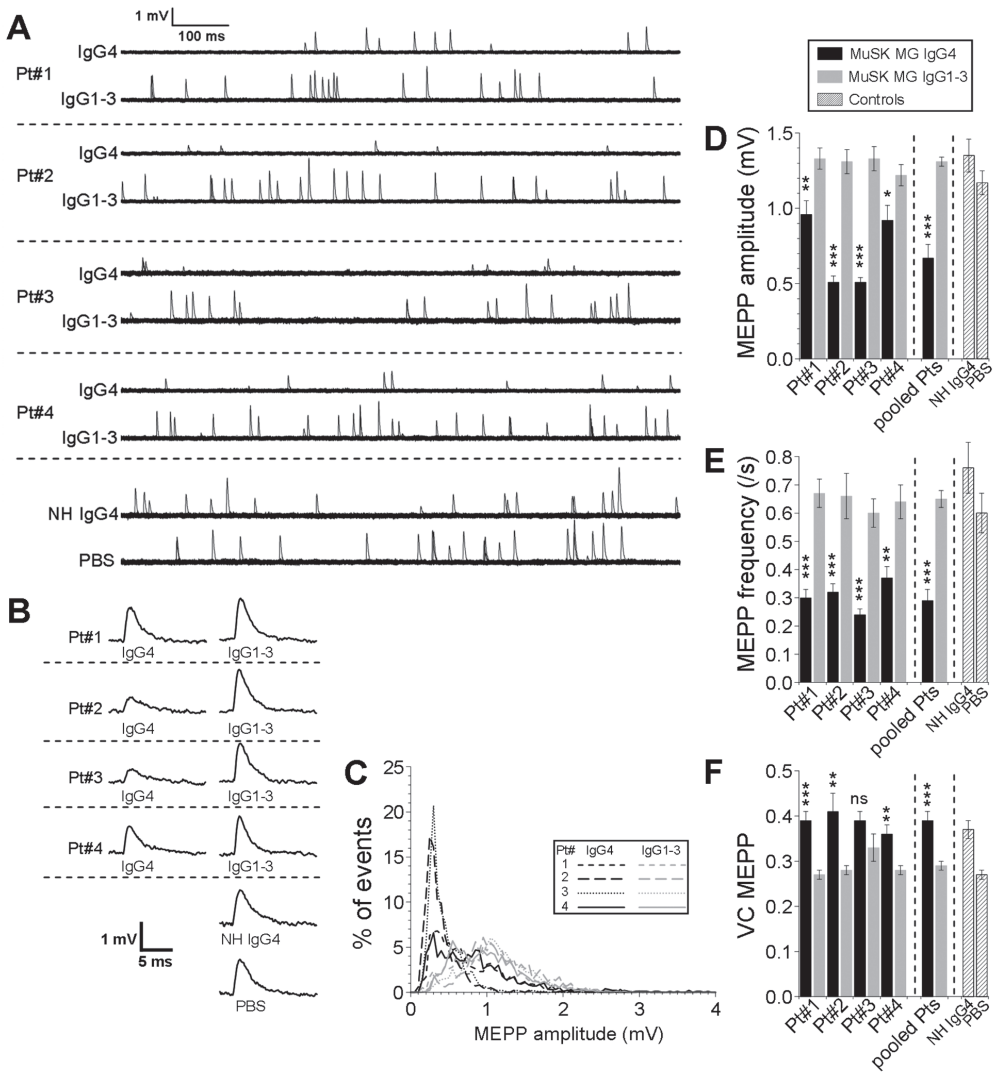

Figure 6. MuSK myasthenia gravis IgG4 causes reduction of the postsynaptic electrophysiological sensitivity for acetylcholine at neuromuscular junctions. *Ex vivo* intracellular electrophysiological microelectrode measurements of miniature endplate potentials at neuromuscular junctions of right hemidiaphragm muscles from passive transfer mice. (A) Examples of 1 s recording traces, 30 traces superimposed. (B) Representative miniature endplate potentials, 15 ms traces. (C) Miniature endplate potential (MEPP) amplitude distributions (based on 896–2316 miniature endplate potentials per condition), showing shift of the miniature endplate potential amplitudes towards smaller values in the neuromuscular junctions from mice treated with MuSK myasthenia gravis IgG4. MuSK myasthenia gravis IgG3 curves were similar to PBS and normal human IgG4 controls (data not shown). Reduced average miniature endplate potential amplitudes (D) and uniquantal spontaneous acetylcholine release, measured as miniature endplate potential frequency (E), at neuromuscular junctions from mouse muscles injected with MuSK myasthenia gravis IgG4. (F) Increased variance coefficient (VC) of miniature endplate potential amplitude at neuromuscular junctions of muscles from mice injected with IgG4 from patients with MuSK myasthenia gravis. Individual patient data in D–F based on 2–4 mice per patient IgG subclass with 8–15 neuromuscular junctions per hemidiaphragm from each

mouse tested; bars represent mean ± SEM of $n = 25–43$ neuromuscular junctions. Pooled patients' bars represent mean ± SEM of $n = 10$ mice treated with MuSK myasthenia gravis IgG4 treated and $n = 8$ mice treated with MuSK myasthenia gravis IgG1–3. *$P < 0.05$, **$P < 0.01$, ***$P < 0.001$, Student's *t*-test, ns = not significant, IgG4 group versus IgG1–3 group. Normal human (NH) IgG4 control bar represents mean ± SEM of 10 neuromuscular junctions from one injected mouse. PBS control bar represents mean ± SEM from 22 neuromuscular junctions from two mice.

10–90% rise times being on average 0.82 ± 0.08 ms with MuSK myasthenia gravis IgG4 and 0.61 ± 0.03 ms with IgG1–3 ($P < 0.05$; supplementary Fig. 1A). In diaphragm from one mouse (Mouse 11, supplementary Table 1) treated with Patient 3 IgG4, 15% of neuromuscular junctions (6 of 40 sampled) showed no miniature endplate potentials at all, and nerve stimulation did not evoke a postsynaptic response. In the other tested muscles, no or only an occasional (<2%) silent neuromuscular junction was encountered, similar to previous observations using our methods in normal, untreated muscles (33). We also recorded endplate potentials at neuromuscular junctions, which result from nerve impulse-induced acetylcholine release from the presynaptic motor nerve terminal. Endplate potentials evoked at 0.3 Hz were considerably smaller at neuromuscular junctions from clinically weak MuSK myasthenia gravis IgG4-treated mice.

The mean amplitude was 16.23 ± 1.25 mV, while the IgG1–3 injected control NOD/SCID group value was 29.23 ± 0.83 mV ($P < 0.001$, Fig. 7A and B) and PBS and normal human IgG4 control values were in the same range (Fig. 7A and B). As with miniature endplate potentials, there was more amplitude variation within individual neuromuscular junctions of patient IgG4-treated mice, showing a mean endplate potential variance coefficient of 0.13 ± 0.01, while the IgG1–3 value was 0.06 ± 0.005 ($P < 0.001$; Fig. 7C), with PBS and normal human IgG4 control values in the same range. Furthermore, there was a tendency of slower endplate potential kinetics, with half-widths and 100–0% decay times being on average 12% increased with MuSK myasthenia gravis IgG4, compared with IgG1–3 ($P < 0.05$; supplementary Fig. 1C and D). From the mean endplate potential (0.3 Hz) and miniature endplate potential amplitudes at each neuromuscular junction we calculated the quantal content (i.e. the number of acetylcholine quanta released per nerve impulse). Surprisingly, in view of the well-known phenomenon of homeostatic upregulation of quantal content when postsynaptic sensitivity for acetylcholine is reduced in myasthenia (34,35,36,37,38), quantal contents at all patient IgG4-treated neuromuscular junctions were similar to all controls, i.e. ~35 quanta per nerve impulse ($P = 0.5$; Fig. 7D). We also stimulated the phrenic nerve at 40 Hz, the approximate physiological firing frequency of rodent motor neurons (39), as used in the tetanic contraction experiments described above. At control neuromuscular junctions, this led to rundown of endplate potential amplitudes to a plateau phase reached after the 10th endplate potential of ~75–80% of the first endplate potential. At neuromuscular junctions of muscles from mice treated with Patients 2, 3 and 4 IgG4, endplate potential run-down was much more

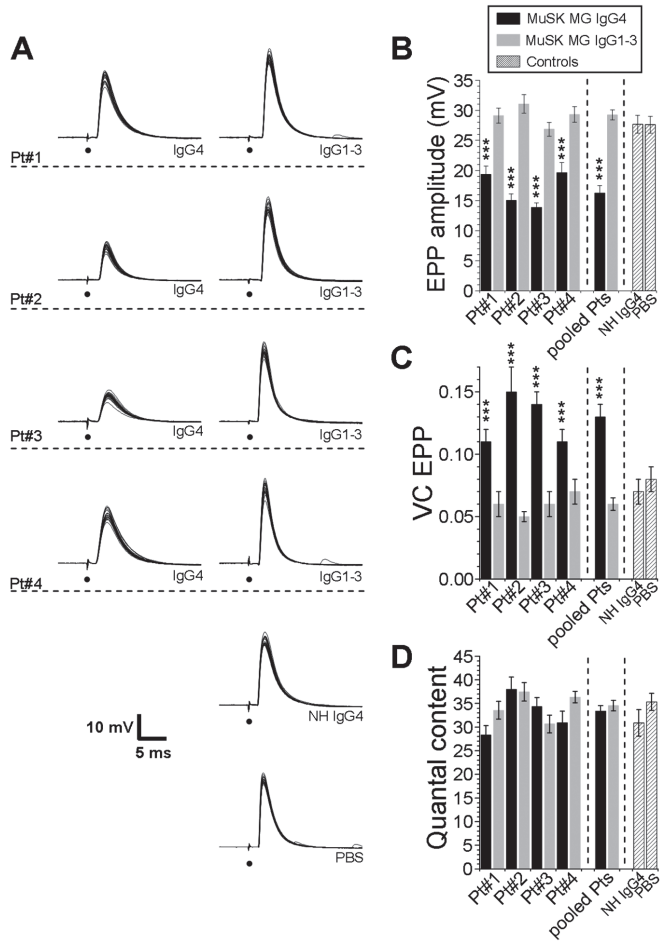

Figure 7. Neuromuscular junctions from mice injected with MuSK myasthenia gravis IgG4 have small endplate potentials and lack compensatory increased acetylcholine release. *Ex vivo* intracellular electrophysiological microelectrode measurements of 0.3 Hz nerve stimulation-evoked endplate potentials at neuromuscular junctions of right hemidiaphragm muscles from passive transfer mice. (A) Exemplary endplate potentials (20 subsequently recorded endplate potentials, superimposed). Black dots indicate the moment of nerve stimulation, causing a stimulation artefact. (B) Mean endplate potential (EPP) values amplitude. (C) Increased variance coefficient (VC) of endplate potential amplitude at neuromuscular junctions of muscles from mice injected with IgG4 from patients with MuSK myasthenia gravis. (D) In spite of reduction of miniature endplate potential amplitude (see Fig. 6), which normally leads to homeostatic increase of acetylcholine release at neuromuscular junctions, neuromuscular junctions of muscles from mice injected with MuSK myasthenia gravis IgG4 do not have increased quantal contents, all being ~35 quanta released per nerve impulse. Individual patient data in B–D based on 2–4 mice per patient IgG subclass with 8–15 neuromuscular junctions per hemidiaphragm from each mouse tested; bars represent mean ± SEM of $n = 25–43$ neuromuscular junctions. Pooled patients bars represent mean ± SEM of $n = 10$ mice treated with MuSK myasthenia gravis IgG4 treated and $n = 8$ mice treated with MuSK myasthenia gravis IgG1–3. ***$P < 0.001$, Student's *t*-test, IgG4 group versus IgG1–3 group. Normal human (NH) IgG4 control bar represents mean ± SEM of 10 neuromuscular junctions from one mouse injected. PBS control bar represents mean ± SEM from 22 neuromuscular junctions from two mice.

pronounced, to a plateau value of 57, 53 and 59%, respectively ($P < 0.001$; Fig. 8A–C). For Patient 1 IgG4, this was not the case. As with 0.3 Hz evoked endplate potentials, there was more amplitude variation amongst subsequent endplate potentials during the plateau phase at individual neuromuscular junctions. While the mean variance coefficient of all controls was 0.08 ± 0.004, the patient IgG4 value was 0.20 ± 0.01 ($P < 0.001$; Fig. 8D). The electrophysiological measurements show that MuSK myasthenia gravis IgG4, but not IgG1–3, causes combined pre- and postsynaptic electrophysiological defects that eventually lead to defective transmission and completely explain the (fatigable) muscle weakness.

MuSK myasthenia gravis IgG1–3 plus additional human complement does not induce muscle weakness

NOD/SCID mice lack an active haemolytic complement system (24), meaning that a potential complement-mediated effect of injected MuSK myasthenia gravis patient IgG1–3 might have been missed. To control this possibility we injected 0.5 ml normal human serum as complement source into NOD/SCID mice pretreated for 10–18 days with 4 mg/day MuSK myasthenia gravis patient IgG1–3 (each of the four patient IgG1–3 tested in one mouse). This treatment paradigm has been shown to cause complement-dependent neuromuscular junction damage in a mouse model for another autoimmune neuromuscular disease, Miller Fisher syndrome (using anti-GQ1b ganglioside antibodies) (33). However, no muscle weakness occurred in the following 3 h, and no CMAP reduction was observed with electromyography. Dissected diaphragms had normal d-tubocurarine sensitivity in contraction experiments and electrophysiological neuromuscular junction parameters were within range of IgG1–3 alone, normal human IgG4- and PBS-injected NOD/SCID control mice (data not shown). This shows there was no substantial *in vivo* binding of MuSK myasthenia gravis IgG1–3 to neuromuscular junctions, confirming the *in vitro* immunofluorescence studies (Fig. 2). Together this excludes complement-mediated effects at the neuromuscular junction of the used MuSK myasthenia gravis IgG1–3.

Disturbed pre- and postsynaptic neuromuscular junction geometry in MuSK-myasthenia gravis IgG4-treated mice

After finishing the functional studies, diaphragms from passive transfer mice were stained for AChRs to enable neuromuscular junction imaging. Confocal laser scanning microscopy of neuromuscular junctions of mice treated with MuSK myasthenia gravis IgG4 showed severe morphological abnormalities (Fig. 9A–I), including very small (~25% of control area, $P < 0.01$, ANOVA, Fig. 9D) and less intensely stained AChR clusters (summed pixel intensity/neuromuscular junction <20% of controls, $P < 0.01$, ANOVA, Fig. 9F). Many neuromuscular junctions had an irregular, dispersed and punctuate staining pattern (Fig. 9G). A proportion of neuromuscular junctions showed remarkable striping, with multiple elongated clusters running in parallel along the longitudinal muscle fibre axis (Fig. 9G). Some neuromuscular junctions showed

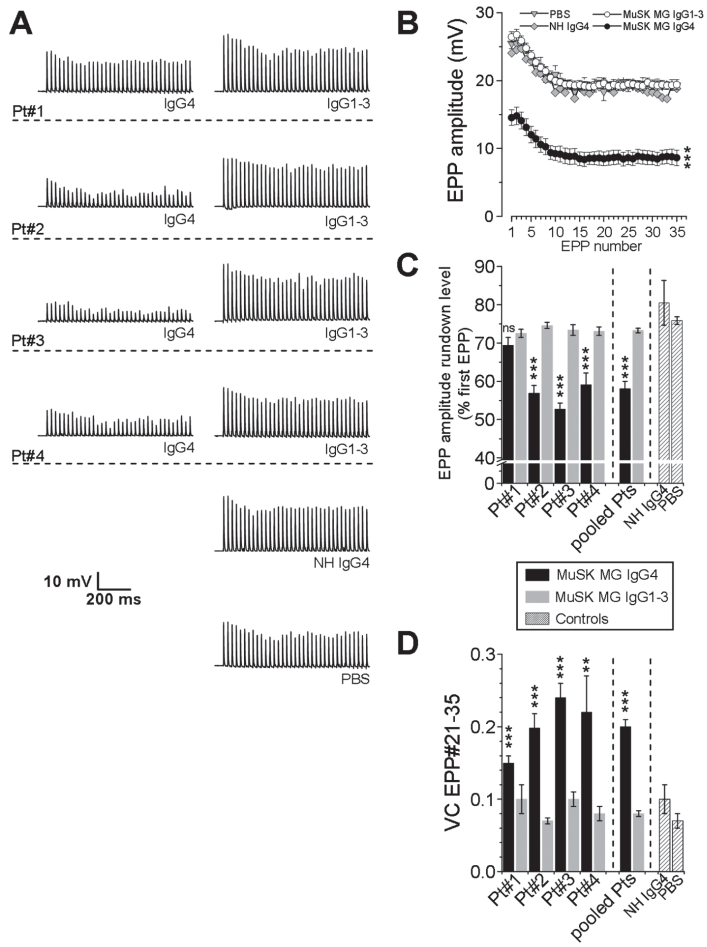

Figure 8. Passive transfer with MuSK myasthenia gravis IgG4 causes extra depression of acetylcholine release during high-rate use of neuromuscular junctions. *Ex vivo* intracellular electrophysiological microelectrode measurements of 40 Hz nerve stimulation-evoked endplate potentials at neuromuscular junctions of right hemidiaphragm muscles from passive transfer mice. (A) Examples of endplate potential trains recorded; 1 s duration traces. Stimulation artefacts have been partially removed for clarity. (B) Average endplate potential (EPP) amplitudes during 35 pulses of 40 Hz nerve stimulation. Pooled data from 10 clinically weak MuSK myasthenia gravis IgG4-injected mice, eight MuSK myasthenia gravis IgG1–3 injected mice, one normal human IgG4-injected mouse and two PBS-injected mice. (C) Mean run-down level is exaggerated at neuromuscular junctions from muscles from mice injected with MuSK myasthenia gravis Patients 2, 3 and 4 IgG4. (D) Neuromuscular junctions from MuSK myasthenia gravis IgG4-injected mice showed more amplitude variation during the plateau phase of the endplate potential trains. Individual patient data in B–D based on 2–4 mice per patient IgG subclass with 8–15 neuromuscular junctions per hemidiaphragm from each mouse tested; bars represent mean ± SEM of $n = 25–43$ neuromuscular junctions. Pooled patients bars represent mean ± SEM of $n = 10$ mice treated with MuSK myasthenia gravis IgG4 treated and $n = 8$ mice treated with MuSK myasthenia gravis IgG1–3. $^{**}P < 0.01$, $^{***}P < 0.001$, Student's *t*-test, IgG4 group versus IgG1–3 group. Normal human (NH) IgG4 control bar represents mean ± SEM of 10 neuromuscular junctions from one mouse injected. PBS control bar represents mean ± SEM from 22 neuromuscular junctions from two mice.

a vague remnant of the normal 'pretzel-like' structure, readily observed at bright intensity in NOD/SCID controls (MuSK IgG1–3, normal human IgG4 and PBS, Fig. 9H and I). In separate imaging experiments on levator auris longus muscles from passive transfer mice we double-stained neuromuscular junctions for AChRs and the presynaptic marker SV2. As with diaphragm from MuSK myasthenia gravis IgG4-treated mice, many AChR clusters in levator auris longus neuromuscular junctions were fragmented, more faintly and punctately stained, again sometimes with vague remnants of a pretzel-like structure. Again, striping was observed at a proportion of the neuromuscular junctions (Fig. 10A). Patient IgG1–3 or normal human IgG4 injected NOD/SCID controls showed more continuous, brightly stained pretzel-like structures (Fig. 10A). SV2 staining in these controls clearly co-localized with AChRs, and was rather continuous.

In MuSK myasthenia gravis IgG4-treated neuromuscular junctions this was less clear, SV2 staining being somewhat more punctuate and co-localized with the vaguely stained remnant of the AChR pretzel-like structure than with the dispersed AChR puncta (Fig. 10A).

Electron microscopic investigation of diaphragm neuromuscular junctions from passively transferred mice confirmed the postsynaptic membrane defects. Many neuromuscular junctions from MuSK myasthenia gravis IgG4-treated mice showed less extensive postsynaptic foldings, the postsynaptic folding index (length of the postsynaptic membrane normalized to the length of the presynaptic membrane) being reduced by ~25%, compared with the neuromuscular junctions from IgG1–3-treated mice ($P < 0.001$, Student's t-test, Fig. 10B and C).

These morphological studies clearly show that MuSK myasthenia gravis IgG4 induces fragmentation and reduction of the postsynaptic AChR area and that presynaptic geometry changes too, albeit less dramatically. It should be realized that the extent of the remaining postsynaptic area may have been overestimated considerably, due to a complete disappearance of a proportion of neuromuscular junctions, especially at diaphragm, as suggested by the electrophysiological measurements and our visual assessments of the AChR immunofluorescence preparations. Overall, the morphological neuromuscular junction defects induced by MuSK myasthenia gravis IgG4 showed much similarity with those observed in active and (whole-IgG) passive MuSK myasthenia gravis mouse models by others (22,23,40,41).

DISCUSSION

IgG4 is traditionally considered as an anti-inflammatory IgG, as opposed to IgG1 and IgG3 subclasses, which activate immune cells and complement. Therefore, the role of elevated and antigen-specific IgG4 in a number of autoimmune diseases has thus far been enigmatic (17,10,15,41). We show here that IgG4 from patients with MuSK myasthenia gravis binds to mouse neuromuscular junctions and causes severe muscle weakness, without requiring other immune system components. Detailed synaptic function analyses showed severely reduced electrophysiological postsynaptic

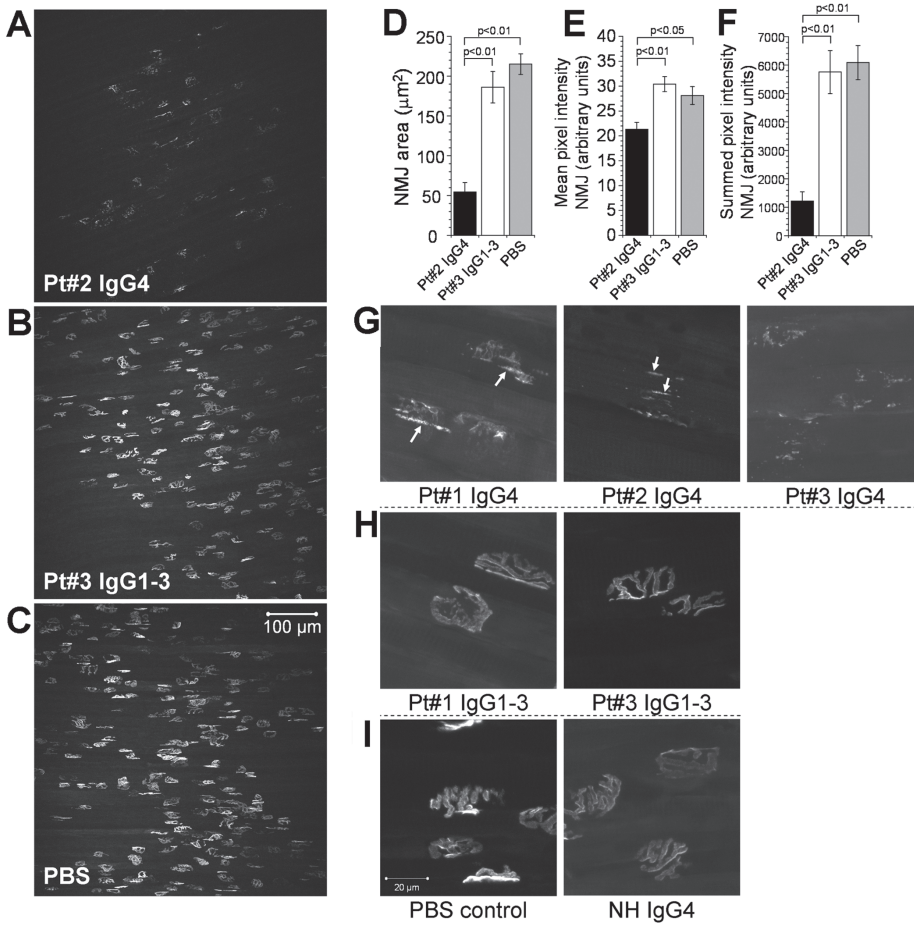

Figure 9. Disturbed postsynaptic neuromuscular junction (NMJ) morphology in MuSK myasthenia gravis IgG4 passive transfer mice. Example confocal laser scanning maximum intensity *z*-stack projections of AChR-stained neuromuscular junctions from mice treated with (A) Patient 2 MuSK myasthenia gravis IgG4, (B) Patient 3 IgG1–3, or (C) PBS. Muscles were processed together in one identical experimental run, allowing direct comparison of area and intensity of staining, which were greatly reduced at MuSK myasthenia gravis IgG4-treated neuromuscular junctions (D–F), mean ± SEM of $n = 10$ random neuromuscular junctions; *P*-value at least < 0.05, ANOVA. (G) Typical stripes (white arrows) were often present at neuromuscular junctions with disintegrated AChR area. (H) Normal AChR staining at example control neuromuscular junctions treated with MuSK myasthenia gravis IgG1–3 treated neuromuscular junctions or (I) normal human (NH) IgG4 or PBS. Scale bar = 100 µm (A, B, C); = 20 µm (G, H, I).

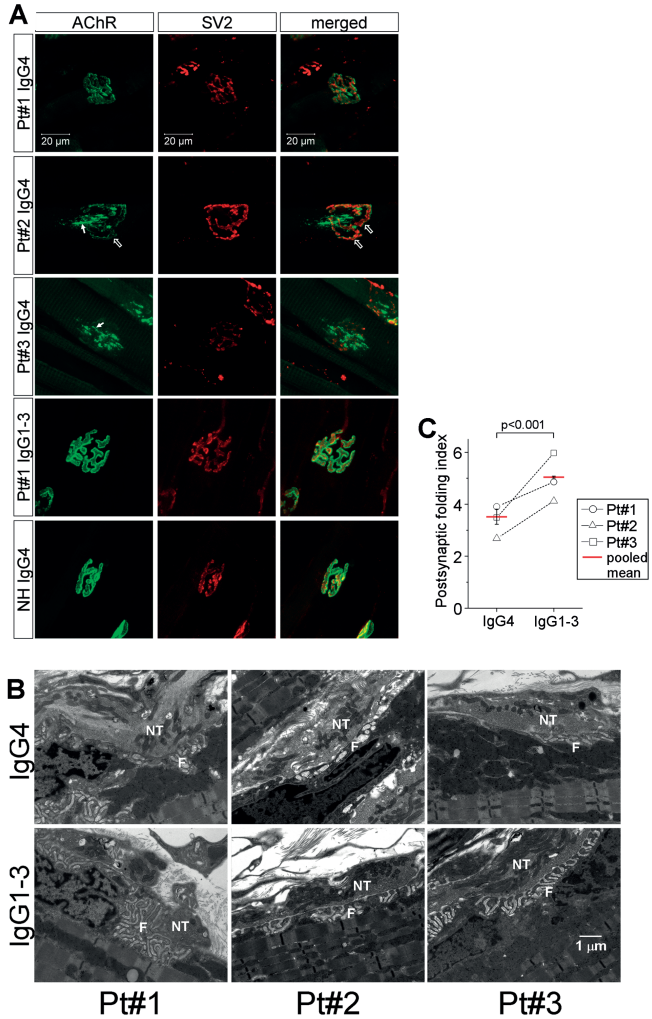

Figure 10. Disturbed presynaptic neuromuscular junction morphology and postsynaptic ultrastructure in MuSK myasthenia gravis IgG4 passive transfer mice. (A) Levator auris longus neuromuscular junctions co-stained for AChRs (green) and presynaptic SV2 (red). Disrupted AChR geometry was present, albeit less outspoken than in diaphragm, especially with Patient 1 IgG4. Striping (white arrows) and vague remnants of normal structure (white hollow arrow) were sometimes encountered. SV2 staining was somewhat more punctuate and dispersed, as compared with control neuromuscular junctions from MuSK myasthenia gravis IgG1–3 or normal human IgG4-treated mice, showing more clear and continuous staining, co-localizing with the clear AChR staining. (B) Ultrastructure of diaphragm neuromuscular junctions showed less extensive postsynaptic foldings. NT = nerve terminal area, F = folding area. Scale bar = 1 µm. (C) Electron microscopy morphometry demonstrates lower folding index (i.e. simplified postsynaptic membranes) at neuromuscular junctions of MuSK myasthenia gravis IgG4-injected mice ($P < 0.001$, pooled mean value of $n = 34$ MuSK myasthenia gravis IgG4 profiles versus $n = 68$ MuSK myasthenia gravis IgG1–3 profiles, Student's t-test).

acetylcholine sensitivity at neuromuscular junctions and an extra rundown of presynaptic transmitter release during intense synaptic activity jointly underlie the weakness. Of particular interest, MuSK myasthenia gravis mouse model neuromuscular junctions lacked compensatory upregulation of acetylcholine release, which is the normal homeostatic presynaptic response to reduced postsynaptic acetylcholine sensitivity. This renders them more vulnerable to transmission block. We are the first to pinpoint human anti-MuSK IgG4 as specific myasthenogenic and to reveal the exact pre- and postsynaptic functional defects it causes at the neuromuscular junction.

Our study clearly demonstrates that MuSK myasthenia gravis IgG4 targets the neuromuscular junction. *In vitro* staining of levator auris longus neuromuscular junctions of normal mice showed binding of IgG4, but not IgG1–3, which entirely co-localized with AChRs. Any unexpected neuromuscular junction binding of IgG4 antibodies per se was excluded in control incubations with purified normal human IgG4. The (fatigable) muscle weakness and ~20–100% electromyographical CMAP decrement observed in clinically weak MuSK myasthenia gravis IgG4-injected mice indicated neuromuscular junction dysfunction. Similar electromyographical observations were made previously in MuSK myasthenia gravis whole-IgG passive transfer mice (22). Fatigable muscle weakness hallmarks (MuSK) myasthenia gravis (42) and, provided testing clinically weak muscles, CMAP reduction is found in most patients with MuSK myasthenia gravis (43). Myasthenia was absent in NOD/SCID control mice receiving either MuSK myasthenia gravis IgG1–3, normal human IgG4 or PBS alone. This shows that MuSK myasthenia gravis IgG4 specifically caused muscle weakness and, together with the correlation of anti-MuSK IgG4 titre with disease severity (14), strongly suggests it is the crucial pathogenic factor in MuSK myasthenia gravis. Earlier studies suggested that anti-MuSK auto-antibodies might only be bystanding disease markers, in view of absence of AChR reduction and IgG deposits at biopsied MuSK myasthenia gravis neuromuscular junctions (20,21). However, subsequent animal studies including this one, strongly suggest anti-MuSK antibody to be the cause. First, post-natal deletion of the MuSK gene in mouse muscle causes severe weakness due to AChR loss at neuromuscular junctions, demonstrating that post-developmental removal of MuSK leads to myasthenia (44). Second, immunization of rabbits (45) or mice (40,41,46) with (rat) MuSK extracellular domain fragments yields paralytic animals with myasthenic features, i.e. CMAP decrement and reduced AChR density at neuromuscular junctions. Third, injection of high doses (45 mg/day) of MuSK myasthenia gravis total-IgG into mice causes myasthenia, also with CMAP reduction and AChR loss (22,23). Local injection of MuSK myasthenia gravis whole-plasma induced subclinical myasthenia in foot muscle (47). Fourth, the weak mice in our present study pinpoint anti-MuSK IgG4 as the crucial myasthenogenic factor. One reason for not observing AChR loss at biopsied human MuSK myasthenia gravis neuromuscular junctions, at least in one study (21), may have been that extremity muscle was used, which is normally not clinically weak in MuSK myasthenia gravis (42).

NOD/SCID mice are immunodeficient and defective in complement ((24)). The induced weakness in them shows that MuSK myasthenia gravis IgG4 can cause myasthenia by itself, without additional immune system components. Complement-independency was already suggested by anti-MuSK antibodies being mainly IgG4 (10,11,12), an IgG subclass unable to activate complement (48), and the observation that complement was not or only scarcely present at biopsied MuSK myasthenia gravis neuromuscular junctions (20,21). Although many MuSK myasthenia gravis sera activate complement in a cellular assay, likely due to some anti-MuSK IgG1 presence (49), injection of human complement in NOD/SCID mice pretreated with either of the four MuSK myasthenia gravis patient IgG1–3 s did not cause weakness here. Collectively, this supports the idea that MuSK myasthenia gravis differs from AChR myasthenia gravis, with AChR antibodies being IgG1 and IgG3 (13), and readily detectable complement at biopsy neuromuscular junctions (19,18). Although MuSK myasthenia gravis IgG1–3 did not cause weak mice, we cannot exclude some contribution in the few patients with MuSK myasthenia gravis with additional anti-MuSK IgG1–3.

We observed some variability in potency amongst MuSK myasthenia gravis IgG4s from different patients (supplementary Table 1), and dose-dependency of effects as exemplified by IgG4 from Patient 2 with low daily doses (0.13 and 1 mg) causing only subclinical myasthenia (detected in muscle contraction experiments using d-tubocurarine), while 4 mg/day induced overt clinical weakness. Others induced weakness in mice with high doses of 45 mg total MuSK myasthenia gravis IgG per day (22). Because IgG4 constitutes between 5% and 14% of total IgG (at least in the MuSK myasthenia gravis sera that were used in our current study; R. Klooster, unpublished data), we estimate this total IgG must have roughly contained 2–6 mg IgG4. This is in the range of the daily doses of purified IgG4 that produced weak mice in the present study and suggests that the effects in the study of (22) were due to the IgG4 component of the injected total IgG.

Electrophysiological study of neuromuscular junctions of MuSK myasthenia gravis IgG4-injected mice revealed clear postsynaptic abnormalities, explaining the muscle weakness. Considerable reductions (~50%) in miniature endplate potential amplitude, indicated greatly reduced AChR density, a hallmark of myasthenic neuromuscular junctions in patients with AChR myasthenia gravis and animal models (34,50,36,37).The faint and fragmented AChR staining observed with confocal fluorescence microscopy, similar to observations in active and passive MuSK myasthenia gravis mouse models by others (22,23,40,41), is compatible with this postsynaptic electrophysiological defect. In further agreement, electron microscopic investigation revealed simplified postsynaptic membrane ultrastructure, as shown in a MuSK myasthenia gravis muscle biopsy (20). Due to the fragmented AChR area, acetylcholine quanta released from different presynaptic sites will act on different local postsynaptic AChR densities. This may explain the higher (miniature) endplate potential amplitude variations at individual neuromuscular junctions. Another factor may be the distribution of the acetylcholine degrading acetylcholinesterase, which

by interaction with perlecan and collagenQ, is determined by MuSK (51). Immune attack on MuSK might create less uniform acetylcholinesterase density in the synaptic cleft and thus local variation of acetylcholine hydrolysis, causing increased (miniature) endplate potential amplitude variation. In addition, the somewhat slower (miniature) endplate potential kinetics we observed may indicate some overall reduction of acetylcholinesterase, because (miniature) endplate potential broadening is a hallmark of acetylcholinesterase inhibition (52,53). Notably, many MuSK patients with myasthenia gravis do not benefit from acetylcholinesterase inhibiting drugs, standard and beneficially used in AChR myasthenia gravis, and may even display symptoms of overdosing when receiving only moderate doses (6,54,55). Collectively, this suggests that AChR reduction at neuromuscular junctions of patients with MuSK myasthenia gravis may be paralleled by (partial) acetylcholinesterase loss. In agreement, very recent active immunization and MuSK myasthenia gravis whole-IgG passive transfer mouse studies showed reduction of acetylcholinesterase protein expression at neuromuscular junctions (56) and acetylcholinesterase messenger RNA at some muscle types (41). Alternatively, changes in (miniature) endplate potential kinetics may result from the disturbed AChR geometry and density by itself, forcing the acetylcholine molecules released to diffuse further to encounter AChR molecules.

One mouse treated with MuSK myasthenia gravis Patient 3 IgG4 had 15% 'silent' neuromuscular junctions, i.e. with no synaptic electrophysiological signals. This agrees with some muscle fibres having barely or no detectable AChRs in confocal microscopy, as also shown by others in MuSK myasthenia gravis total-IgG passive transfer mice (23). Significant numbers of silent neuromuscular junctions were not encountered with IgG4 from the other patients, nor in (weak) muscles from mice injected with lower doses Patient 3 IgG4 (data not shown). This demonstrates that this phenomenon is dose- and patient-dependent, and probably represents the most extreme form of neuromuscular junction disruption by anti-MuSK IgG4. Silenced neuromuscular junctions in the diaphragm of the mouse treated with Patient 3 IgG4 likely also contributed to the lower absolute tetanic contraction force measured *ex vivo*.

The amplitudes of 0.3 Hz nerve stimulation-evoked endplate potentials were severely reduced (on average by ~50%) at neuromuscular junctions of muscles from clinically weak MuSK myasthenia gravis IgG4 injected mice. At many neuromuscular junctions they were smaller than 12 mV, about the minimal endplate potential required to trigger a muscle fibre action potential in rodents (57). At 40 Hz, a physiological rate for rodent neuromuscular junctions (39), endplate potentials at many more neuromuscular junctions became <12 mV due to exaggerated amplitude depression (on average by 42% at MuSK myasthenia gravis IgG4-treated neuromuscular junctions, as compared with only 27% depression in IgG1–3 controls). Thus, subthreshold endplate potentials (either continuous or evolving at high-rate nerve firing) at many neuromuscular junctions explains both the (fatigable) weakness in vivo as well as the low absolute contraction force and tetanic fade of diaphragm

muscles in contraction experiments. Endplate potentials of control mice, without *in vivo* or *ex vivo* weakness, were much larger (>25 mV), demonstrating the large safety factor at healthy neuromuscular junctions (58). The greatly increased d-tubocurarine sensitivity of contraction of MuSK myasthenia gravis IgG4-treated mice diaphragms indicates a severely reduced safety factor at those neuromuscular junctions that still had suprathreshold endplate potentials.

Ex vivo myasthenic features of one mouse injected with Patient 1 IgG4 were the least outspoken, in spite of equal dosing (4 mg/day) as the Patient 2 and 4 IgG4 mice, and even twice that of the Patient 3 IgG4 mouse, which was the most affected. This shows potency variation amongst different MuSK myasthenia gravis IgG4s, as shown for total-IgGs by others (22). However, *in vivo* weakness of this one Patient 1 IgG4 mouse was overt and there was rapid weight loss, suggesting that muscles other than the *ex vivo* investigated diaphragm were more affected. Furthermore, we show clear dose-dependency of MuSK myasthenia gravis IgG4, exemplified by Patient 2 IgG4, which in low-dose (1 mg/day) induced temporary weakness *in vivo* (data not shown) and subclinical myasthenia in *ex vivo* analyses (supplementary Fig. 2).

Besides postsynaptic functional defects, MuSK myasthenia gravis IgG4 also induced presynaptic changes: 55% reduction of spontaneous uniquantal acetylcholine release (miniature endplate potential frequency) and greatly exaggerated depression of acetylcholine release at 40 Hz (resulting in extra endplate potential rundown). The miniature endplate potential amplitude distribution curves (Fig. 6C) excluded that the low miniature endplate potential frequency simply resulted from miniature endplate potentials becoming too small to detect. Rather, low miniature endplate potential frequency may indicate small presynaptic terminal size (59). Indeed, we observed somewhat fainter, more punctuate presynaptic SV2 staining. In agreement, neuromuscular junctions from mice injected with MuSK myasthenia gravis total-IgG showed impaired pre- and postsynaptic apposition, indicating reduced functional presynaptic area (i.e. with opposite AChR presence) (22). In theory, anti-MuSK IgG4 may act directly on the presynaptic motor nerve terminal. However, neuronal MuSK expression is unlikely (4), although it cannot be completely ruled out (60). It is more conceivable that autoimmune attack of postsynaptic MuSK, either directly or indirectly, disturbs functional and structural synaptic homeostasis pathways at neuromuscular junctions. Neuromuscular junctions from patients with AChR myasthenia gravis and rodent models display 50–200% upregulation of acetylcholine release, counteracting postsynaptic AChR loss and involving yet unidentified retrograde signalling factors (36,37,61), and similar synapse homeostasis in response to various challenges is observed in many species (62,63,64,65,66). At neuromuscular junctions of MuSK myasthenia gravis IgG4-injected myasthenic mice we observed failure of this important homeostatic response, aggravating weakness. This suggests a role for MuSK in the underlying pathways that sense AChR loss or release retrograde messaging molecules. Interestingly, some MuSK-signalling pathway members interact with or take part in the postsynaptic dystrophin glycoprotein complex (e.g. agrin and

rapsyn) (67,68,69,70), and deletions from this complex affect neuromuscular junction structure, function and synaptic homeostasis (68,71). Alternatively, lack of appropriate homeostasis at MuSK IgG4-treated neuromuscular junctions may be due to secondary presynaptic damage, merely following the severe postsynaptic disruption, preventing the nerve terminal to respond to retrograde signals. Disturbance of pre- and postsynaptic apposition (22) may be relevant here because if the total nerve terminal would in fact release extra acetylcholine, a partial lack of opposing AChR area would obscure this. The observed increase in endplate potential rundown may be seen as an indication that such 'hidden' quantal content increase indeed exists, causing a more rapid exhaustion of transmitter quanta, which is a feature of myasthenic motor nerve terminals once homeostatic transmitter upregulation is achieved (37). In any case, lack of upregulated functional acetylcholine release at MuSK myasthenia gravis neuromuscular junctions renders transmission more vulnerable to AChR loss, as compared with AChR myasthenia gravis neuromuscular junctions with adequate upregulation.

In conclusion, we provide strong evidence of anti-MuSK IgG4 being the crucial pathogenic factor in MuSK myasthenia gravis, causing combined pre- and postsynaptic functional neuromuscular junction defects with absence of an adequate synaptic homeostatic response, all contributing to muscle weakness. Microelectrode studies of neuromuscular junctions in MuSK myasthenia gravis muscle biopsies agree with the present mouse study: reduced miniature endplate potential amplitude without compensatory increased acetylcholine release (20,72), paralleled by low miniature endplate potential frequency and extra endplate potential rundown (72). This adds clinical relevance to our MuSK myasthenia gravis IgG4 mouse model. The role of IgG4 in MuSK myasthenia gravis as well as in other IgG4-associated autoimmune diseases has hitherto been uncertain (17,15,12,49). So far, only IgG4 (directed against an epidermal protein) in a variant of the autoimmune blistering disease pemphigus has been shown to cause blisters upon intradermal injection of mice (73,74). However, the precise pathological effects were not clarified. We are the first to demonstrate pathogenic action of an IgG4 auto-antibody on the neuromuscular system. The results may provide rationale for selective IgG4 depletion from MuSK myasthenia gravis patient plasma as therapy, rather than the currently practiced total plasmapheresis (75).

REFERENCES

1. Hoch W et al. (2001) Auto-antibodies to the receptor tyrosine kinase MuSK in patients with myasthenia gravis without acetylcholine receptor antibodies. Nat Med 7:365-368.
2. Kim N et al. (2008) Lrp4 is a receptor for Agrin and forms a complex with MuSK. Cell 135:334-342.
3. Linnoila J, Wang Y, Yao Y, Wang ZZ (2008) A mammalian homolog of Drosophila tumorous imaginal discs, Tid1, mediates agrin signaling at the neuromuscular junction. Neuron 60:625-641.
4. Valenzuela DM et al. (1995) Receptor tyrosine kinase specific for the skeletal muscle lineage: expression in embryonic muscle, at the neuromuscular junction, and after injury. Neuron 15:573-584.
5. Zhang B et al. (2008) LRP4 serves as a coreceptor of agrin. Neuron 60:285-297.
6. Evoli A et al. (2003) Clinical correlates with anti-MuSK antibodies in generalized seronegative myasthenia gravis. Brain 126:2304-2311.
7. Farrugia ME et al. (2006) Single-fiber electromyography in limb and facial muscles in muscle-specific kinase antibody and acetylcholine receptor antibody myasthenia gravis. Muscle Nerve 33:568-570.
8. Farrugia ME et al. (2006) MRI and clinical studies of facial and bulbar muscle involvement in MuSK antibody-associated myasthenia gravis. Brain 129:1481-1492.
9. Niks EH et al. (2006) Strong association of MuSK antibody-positive myasthenia gravis and HLA-DR14-DQ5. Neurology 66:1772-1774.
10. McConville J et al. (2004) Detection and characterization of MuSK antibodies in seronegative myasthenia gravis. Ann Neurol 55:580-584.
11. Ohta K et al. (2007) Clinical and experimental features of MuSK antibody positive MG in Japan. Eur J Neurol 14:1029-1034.
12. Tsiamalos P et al. (2009) Epidemiological and immunological profile of muscle-specific kinase myasthenia gravis in Greece. Eur J Neurol 16:925-930.
13. Vincent A, Newsom-Davis J (1982) Acetylcholine receptor antibody characteristics in myasthenia gravis. I. Patients with generalized myasthenia or disease restricted to ocular muscles. Clin Exp Immunol 49:257-265.
14. Niks EH et al. (2008) Clinical fluctuations in MuSK myasthenia gravis are related to antigen-specific IgG4 instead of IgG1. J Neuroimmunol 195:151-156.
15. Nirula A, Glaser SM, Kalled SL, Taylor FR (2011) What is IgG4? A review of the biology of a unique immunoglobulin subtype. Curr Opin Rheumatol 23:119-124.
16. van der Neut KM et al. (2007) Anti-inflammatory activity of human IgG4 antibodies by dynamic Fab arm exchange. Science 317:1554-1557.
17. Aalberse RC, Stapel SO, Schuurman J, Rispens T (2009) Immunoglobulin G4: an odd antibody. Clin Exp Allergy 39:469-477.
18. Engel AG, Lambert EH, Howard FM (1977) Immune complexes (IgG and C3) at the motor end-plate in myasthenia gravis: ultrastructural and light microscopic localization and electrophysiologic correlations. Mayo Clin Proc 52:267-280.
19. Tsujihata M et al. (1989) Diagnostic significance of IgG, C3, and C9 at the limb muscle motor end-plate in minimal myasthenia gravis. Neurology 39:1359-1363.
20. Selcen D, Fukuda T, Shen XM, Engel AG (2004) Are MuSK antibodies the primary cause of myasthenic symptoms? Neurology 62:1945-1950.
21. Shiraishi H et al. (2005) Acetylcholine receptors loss and postsynaptic damage in MuSK antibody-positive myasthenia gravis. Ann Neurol 57:289-293.

22. Cole RN, Reddel SW, Gervasio OL, Phillips WD (2008) Anti-MuSK patient antibodies disrupt the mouse neuromuscular junction. Ann Neurol 63:782-789.

23. Cole RN et al. (2010) Patient autoantibodies deplete postsynaptic muscle-specific kinase leading to disassembly of the ACh receptor scaffold and myasthenia gravis in mice. J Physiol 588:3217-3229.

24. Shultz LD et al. (1995) Multiple defects in innate and adaptive immunologic function in NOD/LtSz-scid mice. J Immunol 154:180-191.

25. Stacy S et al. (2002) Split tolerance in a novel transgenic model of autoimmune myasthenia gravis. J Immunol 169:6570-6579.

26. Kaja S et al. (2007) Severely impaired neuromuscular synaptic transmission causes muscle weakness in the Cacna1a-mutant mouse rolling Nagoya. Eur J Neurosci 25:2009-2020.

27. Magleby KL, Stevens CF (1972) A quantitative description of end-plate currents. J Physiol 223:173-197.

28. McLachlan EM, Martin AR (1981) Non-linear summation of end-plate potentials in the frog and mouse. J Physiol 311:307-324.

29. Murray LM, Gillingwater TH, Parson SH (2010) Using mouse cranial muscles to investigate neuromuscular pathology in vivo. Neuromuscul Disord 20:740-743.

30. Martinez-Martinez P et al. (2007) Overexpression of rapsyn in rat muscle increases acetylcholine receptor levels in chronic experimental autoimmune myasthenia gravis. Am J Pathol 170:644-657.

31. Engel AG, Santa T (1971) Histometric analysis of the ultrastructure of the neuromuscular junction in myasthenia gravis and in the myasthenic syndrome. Ann N Y Acad Sci 183:46-63.

32. Martinez-Martinez P et al. (2009) Silencing rapsyn in vivo decreases acetylcholine receptors and augments sodium channels and secondary postsynaptic membrane folding. Neurobiol Dis 35:14-23.

33. Halstead SK et al. (2008) Eculizumab prevents anti-ganglioside antibody-mediated neuropathy in a murine model. Brain 131:1197-1208.

34. Cull-Candy SG, Miledi R, Trautmann A, Uchitel OD (1980) On the release of transmitter at normal, myasthenia gravis and myasthenic syndrome affected human end-plates. J Physiol 299:621-638.

35. Milone M et al. (1998) Mode switching kinetics produced by a naturally occurring mutation in the cytoplasmic loop of the human acetylcholine receptor epsilon subunit. Neuron 20:575-588.

36. Plomp JJ, van Kempen GT, Molenaar PC (1992) Adaptation of quantal content to decreased postsynaptic sensitivity at single endplates in alpha-bungarotoxin-treated rats. J Physiol 458:487-499.

37. Plomp JJ et al. (1995) Acetylcholine release in myasthenia gravis: regulation at single end-plate level. Ann Neurol 37:627-636.

38. Sandrock AW, Jr. et al. (1997) Maintenance of acetylcholine receptor number by neuregulins at the neuromuscular junction in vivo. Science 276:599-603.

39. Eken T (1998) Spontaneous electromyographic activity in adult rat soleus muscle. J Neurophysiol 80:365-376.

40. Jha S et al. (2006) Myasthenia gravis induced in mice by immunization with the recombinant extracellular domain of rat muscle-specific kinase (MuSK). J Neuroimmunol 175:107-117.

41. Punga AR et al. (2011) Muscle-selective synaptic disassembly and reorganization in MuSK antibody positive MG mice. Exp Neurol 230:207-217.

42. Verschuuren JJ, Palace J, Gilhus NE (2010) Clinical aspects of myasthenia explained. Autoimmunity 43:344-352.

43. Oh SJ et al. (2006) Repetitive nerve stimulation of facial muscles in MuSK antibody-positive myasthenia gravis. Muscle Nerve 33:500-504.

44. Hesser BA, Henschel O, Witzemann V (2006) Synapse disassembly and formation of new synapses in postnatal muscle upon conditional inactivation of MuSK. Mol Cell Neurosci 31:470-480.

45. Shigemoto K et al. (2006) Induction of myasthenia by immunization against muscle-specific kinase. J Clin Invest 116:1016-1024.

46. Xu K, Jha S, Hoch W, Dryer SE (2006) Delayed synapsing muscles are more severely affected in an experimental model of MuSK-induced myasthenia gravis. Neuroscience 143:655-659.

47. ter Beek WP et al. (2009) The effect of plasma from muscle-specific tyrosine kinase myasthenia patients on regenerating endplates. Am J Pathol 175:1536-1544.

48. Bruggemann M et al. (1987) Comparison of the effector functions of human immunoglobulins using a matched set of chimeric antibodies. J Exp Med 166:1351-1361.

49. Vincent A et al. (2008) Myasthenia gravis seronegative for acetylcholine receptor antibodies. Ann N Y Acad Sci 1132:84-92.

50. Elmqvist D, Hofmann WW, Kugelberg J, Quastel DM (1964) An electrophysiological investigation of neuromuscular transmission in myasthenia gravis. J Physiol 174:417-434.

51. Cartaud A et al. (2004) MuSK is required for anchoring acetylcholinesterase at the neuromuscular junction. J Cell Biol 165:505-515.

52. Fiekers JF (1985) Interactions of edrophonium, physostigmine and methanesulfonyl fluoride with the snake end-plate acetylcholine receptor-channel complex. J Pharmacol Exp Ther 234:539-549.

53. Maselli RA, Leung C (1993) Analysis of anticholinesterase-induced neuromuscular transmission failure. Muscle Nerve 16:548-553.

54. Punga AR, Flink R, Askmark H, Stalberg EV (2006) Cholinergic neuromuscular hyperactivity in patients with myasthenia gravis seropositive for MuSK antibody. Muscle Nerve 34:111-115.

55. Guptill JT, Sanders DB, Evoli A (2011) Anti-MuSK antibody myasthenia gravis: clinical findings and response to treatment in two large cohorts. Muscle Nerve 44:36-40.

56. Kawakami Y et al. (2011) Anti-MuSK autoantibodies block binding of collagen Q to MuSK. Neurology 77:1819-1826.

57. Wood SJ, Slater CR (1997) The contribution of postsynaptic folds to the safety factor for neuromuscular transmission in rat fast- and slow-twitch muscles. J Physiol 500 (Pt 1):165-176.

58. Wood SJ, Slater CR (2001) Safety factor at the neuromuscular junction. Prog Neurobiol 64:393-429.

59. Harris JB, Ribchester RR (1979) The relationship between end-plate size and transmitter release in normal and dystrophic muscles of the mouse. J Physiol 296:245-265.

60. Ip FC et al. (2000) Cloning and characterization of muscle-specific kinase in chicken. Mol Cell Neurosci 16:661-673.

61. Sons MS et al. (2006) alpha-Neurexins are required for efficient transmitter release and synaptic homeostasis at the mouse neuromuscular junction. Neuroscience 138:433-446.

62. Davis GW, Bezprozvanny I (2001) Maintaining the stability of neural function: a homeostatic hypothesis. Annu Rev Physiol 63:847-869.

63. Burrone J, Murthy VN (2003) Synaptic gain control and homeostasis. Curr Opin Neurobiol 13:560-567.

64. Magby JP et al. (2006) Single-cell characterization of retrograde signaling by brain-derived neurotrophic factor. J Neurosci 26:13531-13536.

65. van der Plas MC et al. (2006) Dystrophin is required for appropriate retrograde control of neurotransmitter release at the Drosophila neuromuscular junction. J Neurosci 26:333-344.

66. Regehr WG, Carey MR, Best AR (2009) Activity-dependent regulation of synapses by retrograde messengers. Neuron 63:154-170.

67. Apel ED, Roberds SL, Campbell KP, Merlie JP (1995) Rapsyn may function as a link between the acetylcholine receptor and the agrin-binding dystrophin-associated glycoprotein complex. Neuron 15:115-126.

68. Pilgram GS et al. (2010) The roles of the dystrophin-associated glycoprotein complex at the synapse. Mol Neurobiol 41:1-21.

69. Strochlic L, Cartaud A, Cartaud J (2005) The synaptic muscle-specific kinase (MuSK) complex: new partners, new functions. Bioessays 27:1129-1135.

70. Wu H, Xiong WC, Mei L (2010) To build a synapse: signaling pathways in neuromuscular junction assembly. Development 137:1017-1033.

71. Noakes PG et al. (1995) Aberrant differentiation of neuromuscular junctions in mice lacking s-laminin/laminin beta 2. Nature 374:258-262.

72. Niks EH et al. (2010) Pre- and postsynaptic neuromuscular junction abnormalities in musk myasthenia. Muscle Nerve 42:283-288.

73. Rock B et al. (1989) The pathogenic effect of IgG4 autoantibodies in endemic pemphigus foliaceus (fogo selvagem). N Engl J Med 320:1463-1469.

74. Sitaru C, Mihai S, Zillikens D (2007) The relevance of the IgG subclass of autoantibodies for blister induction in autoimmune bullous skin diseases. Arch Dermatol Res 299:1-8.

75. Schroder A, Linker RA, Gold R (2009) Plasmapheresis for neurological disorders. Expert Rev Neurother 9:1331-1339.

SUPPLEMENTARY MATERIAL

Supplementary description of patients

Patient #1. This female patient presented at the age of 26 with intermittent diplopia and ptosis. A few months later, she experienced shortness of breath, dysarthria and mild proximal arm weakness during her work as a ballet teacher. Ten months after onset of symptoms, dysphagia occurred, she lost more than 10% of her body weight, and had to quit working. Antibodies to the AChR were negative. During the next years, she suffered from recurrent episodes with unexplained fatigue, dyspnea, dysphagia and anxiety for which she received long-term psychiatric treatment. Ten years later, she was referred for analysis of an exacerbation of bulbar weakness and dyspnea. She also complained about a dropping head and worsening of symptoms in the course of the day. Examination showed facial weakness, a feeble voice, fatigable neck and proximal arm weakness, but no ptosis or diplopia. Repetitive nerve stimulation electromyography revealed abnormal decrement of CMAP amplitude in two facial and the hypothenar muscles. Stimulated single fiber showed abnormal jitter in the orbicularis oculi muscle. Now, anti-MuSK antibodies could be demonstrated in the absence of anti-AChR antibodies. Forced vital capacity was 87% of predicted. Pyridostigmine was initiated, causing only muscle twitching and cramps. She underwent five courses of plasma exchange. Plasma was frozen for the studies described here. Because no improvement occurred, she was then treated with high dose steroids. Azathioprine caused liver enzyme reaction and was replacement by mycophenolate mofetil with gradual improvement of symptoms. One year later, steroids could be withdrawn and postintervention status was classified as minimal manifestations.

Patient #2. At age 30, being 14 weeks pregnant, this female experienced intermittent diplopia and mild ptosis. Pyridostigmine improved ocular symptoms, although muscle twitching occurred when dosing increased to 60 mg tds. Anti-AChR antibodies were negative. Severe bulbar symptoms started one week after delivery of a healthy boy, i.e. severe ptosis, ophthalmoparesis, facial weakness with a vertical smile and dysarthria. She also developed mild neck weakness but could still raise her arms >3 min. Repetitive nerve stimulation electromyography of hypothenar and trapezius muscles was normal. Stimulated single fiber electromyography of both orbicularis oculi muscles showed markedly increased jitter and blockings. She refused immunosuppressive therapy, despite recurrent exacerbations with dysphagia and severe shortness of breath. Her weight fell from 56 to 43 kg before she accepted high dose prednisone two years after onset. Now symptoms clearly improved and only occasional diplopia, mild nasal speech and slight difficulty in swallowing solid food remained. Symptoms relapsed when she reduced prednisone on her own initiative. In following years, more continuous bulbar weakness and atrophy of the tongue and facial muscles developed. Seven years after onset, she received intravenous IgG

treatment, without effect. By now, serious concerns existed about her weight loss, complicated by paranoid delusions regarding food and body perception. One month later, plasmapheresis was performed, leading to minimal improvement. Tube feeding was initiated, but she refused antipsychotic treatment. Unfortunately, prednisone was stopped and she was readmitted a few months later with severe respiratory insufficiency requiring ventilation, her weight now being only 36 kg. A second plasma exchange, followed by steroids and intravenous IgG, enabled extubation 3 weeks later. Antibodies to MuSK were demonstrated. Plasma from the second treatment was frozen for the present studies.

Patient #3. This male first experienced tiredness and intermittent diplopia at age 54. One month later, stair climbing became difficult. Being a frequent swimmer, he felt unable to keep his head above the water when doing breaststroke for a few minutes. In the evening his eyelids dropped, left more than right. A neurologist also noticed marked facial weakness. Diagnosis of MG was made and oral pyridostigmine treatment initiated. This slightly improved diplopia, but none of the other symptoms, and only in the first week. Antibodies to AChR were negative. One month later, he had progressive shortness of breath and wheezed during inspiration, especially at night. Repetitive nerve stimulation electromyography showed abnormal CMAP decrement in trapezius muscle. Stimulated single fiber electromyography in orbicularis oculi muscle showed increased jitter. Vital capacity was 68-74% of predicted. Anti-MuSK antibodies were positive. High dose prednisone and azathioprine was initiated, initially leading to some improvement of diplopia and dyspnea. However, six months after onset his speech became less intelligible, diplopia persisted during the day and his legs became weaker, requiring holding onto two banisters while stair climbing. In contrast, he experienced no arm weakness. He had lost 7% body weight in one month. Neurological examination showed marked ptosis, ophthalmoparesis, dysarthria and weakness of facial muscles and both neck flexors and extensors. Noticeable was the focal weakness of both hip extensors (MRC 3 range) and the ankle dorsiflexors (MRC 4 range), whereas he could still do 20 squads with some difficulty. Plasma exchange was performed, markedly improving symptoms. Plasma was frozen for the present studies. The quantitative MG score decreased in 10 days from 14 to 4, out of 39. One month later he felt asymptomatic, had regained weight and walked normally. Neurological examination showed only mild ptosis and minimal weakness of ankle dorsiflexors and hip extensors.

Patient #4. This female patient presented with unilateral ptosis, diplopia, dysphagia and mild proximal limb muscle weakness at age 6. Dysphagia led to 17% body weight loss in one month. Repetitive nerve stimulation of thenar muscles showed a decrement of 34%. Anti-AChR antibodies were negative. Oral pyridostigmine was ineffective. After two respiratory crises (vital capacity 55% of predicted), requiring intubation and assisted ventilation, a thymectomy was performed at age 7. She was treated with

prednisone and azathioprine, but had repeated respiratory crises in the following 3 years. She also needed continuous non-invasive ventilation at night between age 7 and 23. At age 10 she was treated for the first time with plasma exchange during a respiratory crisis leading to rapid clinical improvement. At age 13, weekly plasma exchange treatment was initiated. For this purpose an arteriovenous shunt was created in the left forearm. Mycophenolate mofetil was started, prednisone and azathioprine were withdrawn. At age 15, anti-MuSK antibodies were demonstrated. Weekly plasma exchange therapy was continued for 7 years. During these years she had no recurrence of respiratory crisis and she was able to finish high school and an international management study. Mycophenolate mofetil and pyridostigmine were withdrawn at age 19 and 20 respectively. The plasma exchange interval was increased to 2 weeks at age 21 and to three weeks at age 23 without a clinical deterioration. At this age plasma was frozen and used for the present studies. Examination showed mild facial weakness, rhinolalia, tongue atrophy, and a mild proximal muscle weakness.

Table S1. Overview of all passive transfer mice tested in this study. Indicated is the daily dose of i.p. injected purified subclass IgG in mg, whether or not mice developed visible *in vivo* weakness, body weight change during the last three days of passive transfer and change of compound muscle action potential (CMAP) amplitude recorded at 10 Hz nerve stimulation during subcutaneous needle electromyography at the calf muscles in anesthetized mice. NHS=normal human serum; n.d. = not done; n/a= not applicable.

	mouse#	patient#	daily dose (mg)	*in vivo* weakness	body weight change in last 3 days (%)	CMAP change at 10 Hz nerve stimulation (%)
MuSK MG IgG4	1	1	4	yes	-10	-33
	2	1	4	yes	-10	-21
	3	2	0.13	no	+4	+5
	4	2	1	no	+2	-2
	5	2	4	yes	-17	-67
	6	2	4	yes	-18	-26
	7	3	0.13	no	+1	+6
	8	3	0.5	yes	-15	n.d.
	9	3	1	yes	-25	-98
	10	3	1	yes	-20	-45
	11	3	2	yes	-26	n.d.
	12	4	1.5	no	+4	n.d.
	13	4	4	yes	-5	-38
	14	4	6	yes	-22	-84
MuSK MG IgG1-3	15	1	4	no	+3	+3
	16	1	4	no	+5	+3
	17	2	4	no	+5	-1
	18	2	4	no	+2	+5
	19	3	4	no	0	+3
	20	3	4	no	+4	+2
	21	4	4	no	+2	+4
	22	4	4	no	-1	+6
MuSK MG IgG1-3	23	1	4	no	+6	+5
+ NHS at end	24	2	4	no	-2	+4
	25	3	4	no	+3	+3
	26	4	4	no	+6	+2
Normal human IgG4	27	n/a	4	no	+7	-1
PBS	28	n/a	n/a	no	+1	-2
	29	n/a	n/a	no	+4	+4

Table S2. Comparison of the anti-MuSK antibody titres in patient plasma and serum of passive transfer mice. MuSK titres (nM) were determined with radioimmunoassay in the patient plasmas and the sera of the mice (obtained at the end of the experiment), injected with the different IgG fractions purified from the patient plasmas. Anti-MuSK reactivity in the mice was only observed after injection with the MuSK MG IgG4 fractions and not the IgG1-3 fractions. No anti-MuSK antibodies were detected in the serum of the mouse injected with normal human IgG4.

		Anti-MuSK titre (nM)	
Subject	**Patient plasma**	**IgG4-injected mouse serum**	**IgG1-3 injected mouse serum**
Patient #1	6.3	66.4	0.0
Patient #2	39.8	297.5	0.0
Patient #3	28.0	146.4	0.0
Patient #4	n.d.	n.d.	n.d.
Normal human control	0.0	0.0	n.d.

n.d. = not done

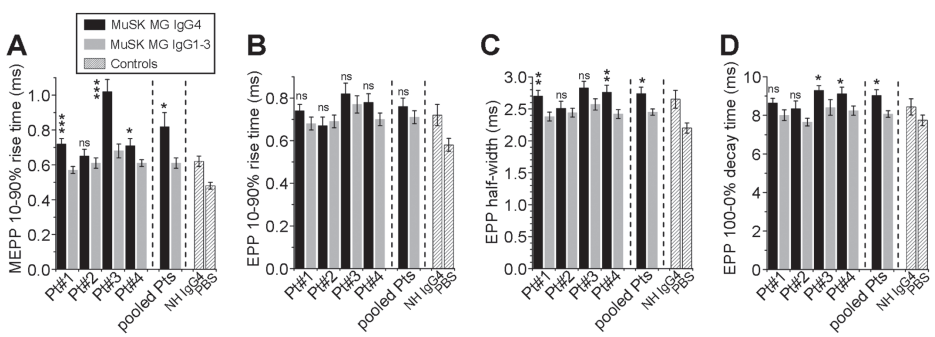

Figure S1. Tendency of slower kinetics of electrophysiological synaptic signals recorded at NMJs from mice injected with MuSK MG IgG4. *Ex vivo* intracellular electrophysiological micro-electrode measurements of MEPPs at NMJs of right hemidiaphragm muscles from passive transfer mice. (A) Rise times of MEPPs showed tendency of increase, especially at NMJs from the diaphragm muscle from the mouse treated with MuSK patient #3 IgG4. (B) Rise times of EPPs were similar in IgG4 and IgG1-3 treated NMJs. (C) EPP width at half the peak height tended to be larger at IgG4-treated NMJs, as well as the time needed to decay from 100 to 0% of the peak amplitude (D). These tendencies for slower MEPP and EPP kinetics at NMJs from MuSK MG IgG4 treated NMJ may point towards reduced presence of acetylcholinesterase in the synaptic cleft (see Discussion). Individual patient data based on 2-4 mice per patient IgG subclass with 8-15 NMJs per hemidiaphragm from each mouse tested; bars represent mean ± S.E.M. of n=25-43 NMJs. Pooled patients bars represent mean ± S.E.M. of n=10 mice treated with MuSK MG IgG4 treated and n=8 mice treated with MuSK MG IgG1-3. *p<0.05, **p<0.01, ***p<0.001, Student's t-test, n.s.=not significant, IgG4 group vs. IgG1-3 group. Normal human (NH) IgG4 control bar represents mean ± S.E.M. of 10 NMJs from one mouse injected. PBS control bar represents mean ± S.E.M. from 22 NMJs from two mice.

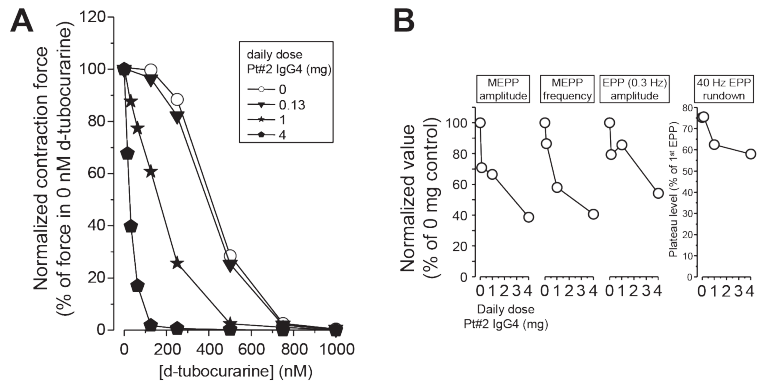

Figure S2. Dose-dependency of the (subclinical) MG induced by passive transfer of MuSK MG patient #2 IgG4. Three mice received either 0.13, 1 or 4 mg/day MuSK MG IgG4 for 38, 32 and 12 days, respectively. Only the mouse injected with 4 mg/day showed overt muscle weakness. (A) In *ex vivo* contraction measurements of their diaphragms there was a dose-dependent increase in the sensitivity of the contraction to d-tubocurarine, indicated by the leftward shift of the concentration-effect curves compared to the control curve which was composed from the pooled data of the MuSK MG IgG1-3, normal human IgG4 and PBS controls of Figure 5B. (B) Similarly, the changes of electrophysiological parameters MEPP amplitude, MEPP frequency, EPP amplitude and EPP rundown induced by the MuSK MG patient #2 IgG4 were dose-dependent.